Physics of the Solid State, Vol. 42, No. 5, 2000, pp. 788–809. Translated from Fizika Tverdogo Tela, Vol. 42, No. 5, 2000, pp. 770–790.

REVIEW

Effects of Strong Electron Correlations in X-ray and Electron Spectra of High-T_c Superconductors

P. V. Avramov and S. G. Ovchinnikov

Kirenskiĭ Institute of Physics, Siberian Division, Russian Academy of Sciences, Akademgorodok, Krasnoyarsk, 660036 Russia

e-mail: paul@post.krascience.rssi.ru

Received in final form November 15, 1999

Abstract—The current state of theoretical and experimental studies on the electronic structure of high-T_c superconductors is analyzed. The agreement between the theory and experimental spectroscopic data is shown to be rather poor in certain cases. The reason is that the X-ray and electronic spectra reveal strong electron correlations. At the same time, no realistic model has been developed up to now in which both one-electron and multielectron mechanisms of the formation of the spectra could be described in a unified way in compounds containing transition and rare-earth elements. In this paper, particular attention is paid to a sudden-perturbation model, by which it has been possible to describe or interpret some X-ray and electronic spectra, including both one-electron and multielectron effects. © *2000 MAIK "Nauka/Interperiodica".*

INTRODUCTION

It can now be confidently said that the discovery of high-T_c superconductivity (HTSC) has given vigorous impetus to the development of many areas of both experimental and theoretical physics. Particularly striking is the development of high-resolution electron spectroscopy and the theory of strong electron correlations. The first attempts to elucidate the features of the electronic structure of high-T_c superconductors and to correlate them with the nature of the HTSC were made almost immediately after the discovery of these compounds [1]. It became clear that the spectral data obtained by X-ray and electron spectroscopy methods could not be unambiguously interpreted. The reason was that the atomic and electronic band structures of the HTSC materials were complicated and also that the spectra showed the effects of strong electron correlations [2–4].

Detailed analysis of the literature concerned with experimental and theoretical studies on high-T_c superconductors shows that a great deal of information on their electronic structure has been accumulated to date. This information was obtained mainly by experimental methods, namely, by X-ray electron and photoelectron spectroscopy, X-ray spectroscopy, X-ray emission spectroscopy, X-ray absorption spectroscopy, and optical spectroscopy.

Photoelectron spectroscopy of core electron states allowed one to obtain some information about more general characteristics of the electronic structure, such as the oxidation levels of copper and the occupancies of multielectron configurations due to strong electron correlations. The X-ray absorption spectra (XASs) also suggest that strong electron correlations affect the electronic structures of high-T_c superconductors, in particular, the structure of unoccupied electronic states in them.

Also, theoretical one-electron calculations of the electronic structure of key objects were made, which were not accompanied, as a rule, by the theoretical modeling of relevant spectroscopic experiments. Only some features of physical experiments, predominantly of those on metallic phases, were adequately described in terms of the theoretical one-electron models developed thus far.

On the other hand, multielectron models of HTSC (the Anderson model, several versions of the Hubbard model, the *t–J* model, etc.) undoubtedly gave some insight into the role of strong electron correlations. However, one-electron excitations of a system were not theoretically treated in these models, which does not allow one to directly compare the theory with the great bulk of the experimental data.

In fact, the view of the electronic structure of high-T_c superconductors has been fragmentary up to now; some effects have been investigated only in one-electron models and others only in multielectron ones. No realistic model was developed, in terms of which one could interpret a great body of experimental data revealing both one-electron and multielectron effects (for example, X-ray absorption spectra and various electronic spectra).

1063-7834/00/4205-0788$20.00

1. BASIC DATA ON THE ELECTRONIC STRUCTURE OF HIGH-T_c SUPERCONDUCTORS

1.1. Electronic Spectra of Superconductors

Analysis of the literature [3, 5–13] shows that Cu2*p* X-ray photoelectron spectra (Cu2*p*-XPSs) of copper were investigated the most, because they can be experimentally measured quite easily. From these spectra, one can obtain some information about the valence and charge states of copper in compounds. Figure 1 shows typical Cu2*p*-XPSs of compounds CuO, $La_{2-x}Sr_xCuO_4$ ($x = 0, 0.15$), and Cu_2O [3, 5]. In the spectra of CuO and $La_{2-x}Sr_xCuO_4$, in contrast to those of Cu_2O, there are two intense peaks, which the authors of [3, 5] associate with transitions to $3d^{10}$ and $3d^9$ states, respectively. The $3d^9$ peak has a complex structure due to the Coulomb interaction of 2*p* and 3*d* vacancies in the final state; this peak is nearly rectangular in shape for "good" samples (fabricated under certain conditions). In the process of physical degradation of the samples, the $3d^9$ peak first becomes asymmetric and then less intense.

The satellite structure of Cu2*p*-XPSs was widely used to estimate the charge distribution in the ground state [14, 15]. Most of the estimations, made in the Anderson model (described in [16–22]) using experimental data, show that, in CuO and $La_{2-x}Sr_xCuO_4$ oxides, the weight of the $3d^9$ configuration does not exceed 50–60% and only a moderate contribution is observed from the $3d^8$ configuration.

There are a number of papers in which the Cu2*p*-XPSs are misinterpreted. In most of the papers, it was concluded that the Cu(+3) ions make a considerable contribution to the chemical bond. Theoretically, we believe that the spectra of the ions in the $NaCuO_2$ compound [23] (Fig. 2), in which the local structural parameters of the environment of the copper ion (CuO_4 cluster) are close to those in the HTSC compounds under study, are of greatest interest. There are two fundamental distinctions between the Cu2*p*-XPS of $NaCuO_2$ and those of La_2CuO_4 and CuO: a noticeable shift of the principal peak and its satellite to shorter wavelengths and the emergence of an additional long-wavelength satellite at an energy of 937.5 eV.

The presence of a complex satellite structure in all the X-ray electron spectra mentioned above is an unambiguous manifestation of strong valence electron correlations in high-T_c superconductors.

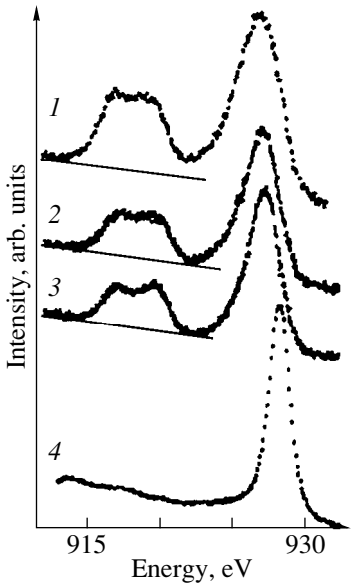

Fig. 1. Cu2$p_{3/2}$ X-ray photoelectron spectra [3, 5] of compounds (*1*) CuO, (*2*) $La_{1.85}Sr_{0.15}CuO_4$, (*3*) La_2CuO_4, and (*4*) Cu_2O.

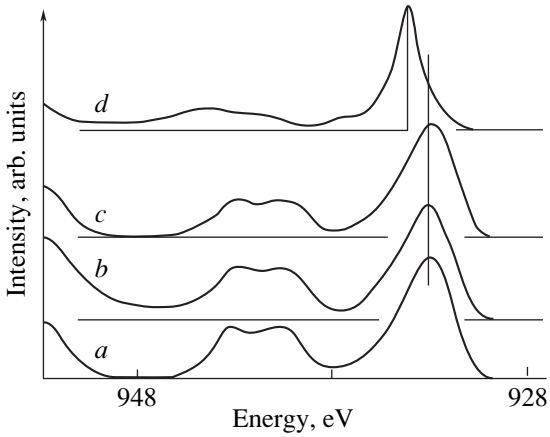

Fig. 2. Cu2$p_{3/2}$ X-ray photoelectron spectra [23] of compounds (*a*) CuO, (*b*) La_2CuO_4, (*c*) $YBa_2Cu_3O_7$, and (*d*) $NaCuO_2$. The half-width of the spectral line Γ(eV) is (*a*) 3.25, (*b*) 3.30, (*c*) 3.20, and (*d*) 1.60.

1.2. X-ray Absorption Spectra of High-T_c Superconducting Compounds

The best understood X-ray absorption (XAFS) spectra of HTSC compounds are Cu*K* spectra. They are observed when X-rays induce transitions of 1*s* electrons of copper to unoccupied Cu*p* orbitals. In copper oxides, there are no vacant Cu*p* states up to the ionization threshold. For this reason, in this energy range, there are no intense lines in all Cu*K* spectra of HTSC compounds and related oxides. Historically [1], the Cu*K* absorption spectra were used, first of all, for determining the oxidation level of copper in high-T_c superconductors. In fact, it was on the basis of these spectra that the erroneous inference was first made that Cu(III) ions are of considerable importance in forming the electronic structure of La_2CuO_4. Later, the nature of the principal peaks of the near-range fine structure of X-ray absorption spectra was elucidated on the basis of one-electron calculations [24–27]. The features of the spectra were identified that are associated with the scatter-

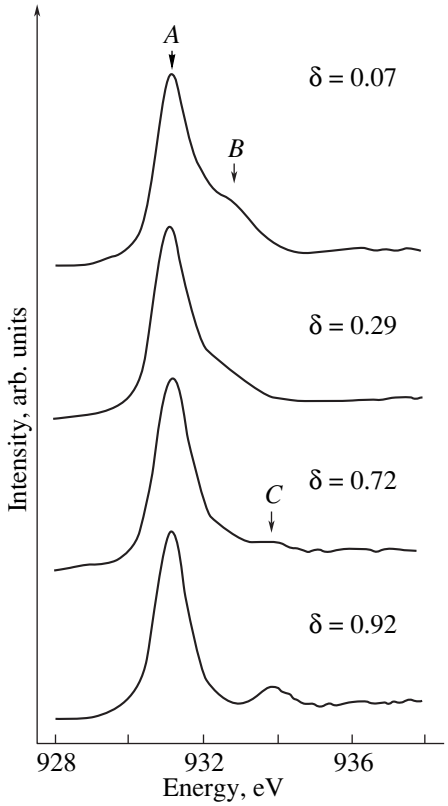

Fig. 3. Experimental CuL_3 X-ray absorption spectra [31] of the $YBa_2Cu_3O_{7-\delta}$ compound for different values of δ.

ing of photoelectrons by the atoms of the first coordination shell [1, 24] and by more distant atoms [25–27].

Noteworthy is the paper by Li *et al.* [26], in which the experimental spectrum was compared with theoretical one-electron calculations of polarized Cu*K* spectra for an extended cluster and the conclusion was drawn that the peak 7 eV higher than the principal peak in the *z*-polarized spectrum has a multielectron nature. However, this hypothesis was not substantiated in [26], not even qualitatively. The Cu*K* spectra are well reproduced, and hence, their variations with composition and under different conditions can be determined with a high degree of accuracy. In the experimental work by Kosugi *et al.* [28], owing to this property of Cu*K* spectra, the spectra of two-hole Cu*p* states were first obtained for doped $La_{2-x}Sr_xCuO_4$ and $YBa_2Cu_3O_7$ compounds. It should be emphasized that work was very important, because only the method proposed in [28] made it possible to separate the spectra corresponding to the electronic states produced by doping.

Another experimentally well studied spectrum of HTSC compounds is the CuL_3 spectrum. The CuL_3 X-ray absorption spectra are associated with the transition of an electron, excited by an X-ray quantum, from the 2*p* energy level of copper either to a *d*-type bound state or to the *s* or *d* orbital in the positive-energy range (after which the electron leaves the system).

Up to now, the mechanism of the formation of CuL_3 X-ray absorption spectra of high-T_c superconductors has been studied either by a method based on the one-electron approximation and multiple-scattering theory (see, e.g., [2, 27]) or by a multielectron treatment based on the Anderson model [29]. The former approach ignores the effects of strong electron correlations, which are important in forming these spectra, while the latter gives a very rough picture of X-ray absorption, reducing the entire spectrum to a single white line and not allowing one to describe the intricate part of the spectrum above the ionization threshold. Nevertheless, some interesting results were obtained using even this much-simplified multielectron description of the formation of CuL_3 X-ray absorption spectra. In [29], the modeling of the white line (transitions to vacant Cu*d* bound states from the core Cu2*p* orbitals) of CuL_3 absorption spectra was performed for both one-hole and two-hole configurations of the CuO_4 cluster in terms of the three-band *p–d* model. It was shown that the *z*-polarized spectrum becomes noticeably more intense after doping. A comparison between the results obtained in [29] and [30] shows that the theory agrees well with the experimental X-ray absorption data; hence, the conclusion is substantiated that the density of Cud_{z^2} states becomes significantly higher after doping.

Nowadays, there is a great body of experimental data [29, 31] suggesting that, in copper-containing HTSC oxides, the mechanisms of the formation of Cu$L_{2,3}$ spectra are essentially different from those described by a one-electron, crystal-field model. First of all, the experimental spectra indicate that there occur electron transitions, known as nondiagrammatic, to the states that cannot be described by this model. These transitions are associated either with strong electron correlations or with photoelectron scattering on possible potential barriers produced by surrounding atoms and chemical bonds in the compounds under discussion. The discrepancies were best demonstrated in [31] in the CuL_3 spectrum of $YBa_2Cu_3O_{7-\delta}$ (Fig. 3).

In [31], the fundamental peak *A* of the white line was attributed to the transition $Cu2p^63d^9 \longrightarrow Cu2p^53d^{10}$ for any value of δ, while the peak *B* for δ = 0.07–0.30 was ascribed to the transition $Cu2p^63d^9\underline{L} \longrightarrow Cu2p^53d^{10}\underline{L}$, accompanied by strong electron-correlation effects, which agrees with the theoretical results obtained in [32], where X-ray absorption due to transitions from the core 2*p* energy level of copper was investigated in the $YBa_2Cu_3O_{7-\delta}$ compound using the Anderson model. When δ is increased (causing the electron vacancy concentration to decrease), the intensity of the peak *B* falls to zero and a peak *C* appears at a distance of 2.8 eV from it. The peak *C* was attributed in [31] (taking into account the position of the fundamental peak in the CuL_3 spectrum of

Cu_2O [33]) to copper ions with the (+1) oxidation level. Undoubtedly, this interpretation of the peak *C* deserves attention, but the mechanism of the formation of the CuL_3 spectrum of univalent copper was not discussed in [31] and [33]. Moreover, the absolute values of the absorption oscillator strengths for the 2*p* orbital of copper in $YBa_2Cu_3O_{7-\delta}$ and Cu_2O were not presented in [33], which does not allow one to correctly analyze the CuL_3 spectrum of the complex $YBa_2Cu_3O_{7-\delta}$ system, which is a combination of the spectra of copper ions with +1, +2, and +3 oxidation levels. Thus, it looks as if, even with allowances made for the multielectron effects, one cannot explain all features of the CuL_3 spectra of copper-containing HTSC materials.

According to [32], in the undoped system (with one electron vacancy per formula unit), X-rays can induce only transition $2p^6d^9_{x^2-y^2} \longrightarrow 2p^5d^{10}$, even though in the initial state there are two d^9 and two $d^{10}\underline{L}$ configurations, due to the hybridization of the vacant states. In doped systems (with more than one vacancy per formula unit), there appear contributions from the Cud^8, Cu$d^9\underline{L}$, and Cu$d^{10}\underline{LL}$ configurations and, hence, the multielectron effects are much stronger. For this reason, the CuL_3 spectra of dopant-produced electronic states of doped compounds noticeably differ from the spectra for undoped ones; in particular, there appear shakeup satellites near the white line [2, 32, 33].

1.3. X-ray Spectra of Core Energy Levels

Nowadays, there is a great body of spectral data available in the literature (see, e.g., [34, 35]) on CuK_α X-ray spectra (transitions from the Cu2*p* to the Cu1*s* orbital ionized by an X-ray quantum). In most of the papers dealing with the theoretical and experimental investigation of these spectra, some spectral features are explained in terms of the Anderson model or the two-band Hubbard model. The mechanisms of the formation of the spectra are commonly discussed for the one-hole configuration, and no account is taken of the contribution from the two-hole configuration, for which the correlation effects are of fundamental importance.

The authors of papers [36, 37] considered the energy shift of the principal peak in the CuK_α spectra that is caused by the phase transition from the nonsuperconducting to the superconducting state in HTSC oxides, among them $La_{2-x}Sr_xCuO_4$. It was shown that only in $YBa_2Cu_3O_7$, the principal peak of the CuK_α spectrum is shifted by 0.35 eV, due to a change of the leading configuration. Theoretically calculated spectra of systems with a one-hole configuration were described in detail in [36, 37]. A low-intensity satellite was shown to exist which depends on the density of states of the Cud^9 configurations and whose position is higher by 0.4 eV than that of the principal peak; the latter depends on the density of the Cu$d^{10}\underline{L}$ state in the 1*s* and 2*p* hole configurations. It was shown in [37] that the shift of the K_α line of copper cannot be measured without separating out the contributions of the satellite structure. Hence, analysis of these spectra cannot be performed without resorting to multielectron methods.

1.4. One-Electron Calculations of the Electronic Structure of Cuprates

Even the first attempts to describe the electronic structure of copper-containing HTSC materials by nonempirical, cluster, and band, one-electron methods were accompanied, as a rule, by comparing the calculations and experimental photoelectron and X-ray emission spectra of these compounds (see, e.g., [1–7, 38–43]). These calculations gave practically the same picture of the electronic structure formed by the Cu3*d* and O2*p* orbitals (see Fig. 4 and, e.g., [44, 45]).

However, it immediately became obvious that there are fundamental limitations to such calculations when applied to HTSC materials.

(1) First of all, the one-electron calculations give zero magnetic moment for copper ions, whereas the experiment shows that all undoped HTSC compounds are antiferromagnets, with the copper ion magnetic moment being equal to $\mu \sim 0.5\mu_B$, and although the high-T_c superconductors themselves possess no long-range antiferromagnetic order, they show strong spin fluctuations [46].

(2) The experimental photoelectron spectra are shifted to lower energies by about 1–2 eV as compared

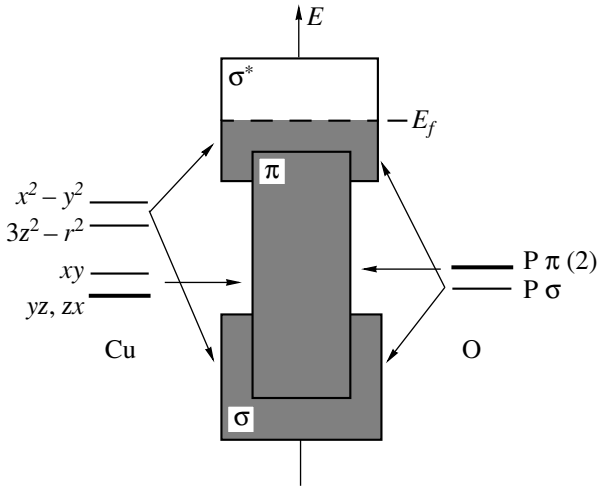

Fig. 4. Schematic diagram of the electronic states of the Cu3*d* and O2*p* orbitals of the CuO_2 plane in terms of the crystal-field theory and its interpretation in terms of the LCAO–LDA method [44, 45]. The hatching shows the occupied states; $\sigma^{(*)}$ and π designate (anti)bonding $pd\sigma$ states.

to the band calculations for both $La_{2-x}Sr_xCuO_4$ and $YBa_2Cu_3O_{7-\delta}$.

(3) The one-electron calculations predict a metallic behavior for the ground state of undoped oxides such as La_2CuO_4 and $YBa_2Cu_3O_6$, whereas the experiment shows that they are insulators.

(4) The one-electron models offer no explanation of X-ray electron spectra and X-ray spectra of the core energy levels of copper and oxygen, because they have a complex satellite structure.

(5) A comparison of the theory and the experiment showed that a number of features of the X-ray absorption spectra of copper also cannot be explained in terms of a simple one-electron model.

In more recent papers [47–49], an attempt has been made to improve the one-electron approach by introducing a vacant-state potential correction. In effect, such a correction to the potential is analogous to the introduction of the parameter U_d in the Hubbard model, which will be discussed below.

This improved approach allowed one to qualitatively explain the forbidden gap, the shift of the photoelectron spectra to lower energies, and the magnetic moment of copper atoms in the ground state of undoped oxides, such as La_2CuO_4, $CaCuO_2$, $Sr_2CuO_2Cl_2$, and $YBa_2Cu_3O_6$. The nature of the electronic states of the top of the valence band and the bottom of the conduction band was also adequately described and the results agreed with the most reliable experimental and theoretical data. Unfortunately, in those papers, modeling of the X-ray and photoelectron spectra was not conducted and a comparison of the calculations and the experimental data was made only indirectly, which does not allow one to definitively judge the adequacy of this approach.

1.5. Strong Electron Correlations

As mentioned above, the one-electron models cannot describe the features of the electronic structure of undoped cuprates and some of their physical and spectral properties associated with strong electron correlations. To take these correlations into account, two methods were used in the literature. One of them is based on models like the Hubbard or the Anderson model, and the other is an *ab initio* approach, such as the configuration interaction (CI) method or the multiconfiguration self-consistent field (MC SCF) approximation.

Model calculations are the simplest and physically most illustrative method for taking strong electron correlations into account. The simplest of them is the tight-binding model, which describes the electronic structure of the CuO_2 plane and takes into account only the atomic orbitals of the CuO_4 cluster (two occupied $p_{x,y}$ orbitals of oxygens and one half-filled $Cud_{x^2-y^2}$ orbital). The corresponding model Hamiltonian has the form

$$H^0_{3bd} = \varepsilon_d \sum_{i,\sigma} d^+_{i\sigma} d_{i\sigma} + \varepsilon_p \sum_{j,\sigma} p^+_{j\sigma} p_{j\sigma}$$

$$+ \sum_{\langle i,j\rangle\sigma} t^{ij}_{pd}(d^+_{i\sigma} p_{j\sigma} + \text{H.c.}) + \sum_{\langle i,j'\rangle\sigma} t^{jj'}_{pp}(p^+_{j'\sigma} p_{j\sigma} + \text{H.c.}).$$

Here, the summation is carried out over atoms in the cluster, $\langle i, j\rangle$ means that the summation is performed over its nearest neighbors, and σ is a spin index. In this model, there are three bands containing five electrons. In actual practice, however, this Hamiltonian is written in the hole representation, in which the state $Cu3d^{10}2O2p^6$ is taken as the vacuum state. In the case of one vacancy, the electronic structure of the CuO_2 plane is reduced to one Hubbard band $Cu3d^9 2O2p^6$. As is customary in this model, $d^+_{i\sigma}$ and $p^+_{j\sigma}$ are the creation operators for holes at d and p orbitals, respectively, of copper and oxygen atoms in the CuO_2 plane. The charge-transfer gap Δ equals the difference between the energies of the p and d states of oxygen and copper ($\Delta \equiv \varepsilon_p - \varepsilon_d$) and is positive in the hole representation. The hopping integrals t^{ij}_{pd} and $t^{jj'}_{pp}$ are parameters of the system, determined either from the experimental data or from some nonempirical calculations. The signs of these parameters are dictated by the symmetry of the system, and their absolute values are much less than Δ ($t^{ij}_{pd}, t^{jj'}_{pp} \ll \Delta$).

This model ignores one of the main features of the strongly localized d orbitals of copper, their strong Coulomb interaction. The Emery model is not subjected to this drawback. It is a three-band analog of the one-band Hubbard model,

$$H_{3bd} = H^0_{3bd} + U_d \sum_i n^d_{i\uparrow} n^d_{i\downarrow}$$

$$+ U_p \sum_j n^p_{j\uparrow} n^p_{j\downarrow} + U_{pd} \sum_{\langle i,j\rangle} n^d_i n^p_j,$$

where $n^d_{i\sigma} = d^+_{i\sigma} d_{i\sigma}$ and $n^p_{j\sigma} = p^+_{j\sigma} p_{j\sigma}$ are the densities of $Cu3d$ and $O2p$ holes, respectively. The quantities U_d and U_p are the Hubbard interaction parameters at the same orbitals for copper and oxygen, respectively, and U_{pd} characterizes the copper–oxygen interaction. In the hole representation, these quantities are positive and correspond to repulsion. The quantity U_d is dominant in the formation of the electronic structure and because of this, the transition $Cu3d^9 \longrightarrow Cu3d^8$ is suppressed.

The limit case where all three Hubbard interaction parameters are zero ($U_d = U_p = U_{pd} = 0$) corresponds to one-electron calculations. In this case, the upper σ^*

band (Fig. 4) is twofold degenerate (in terms of this model) and, hence, half-filled.

As the Hubbard repulsion parameter U_d increases, the degeneracy of the σ* band is lifted and there appear the lower (LHB) filled and the upper (UHB) vacant Hubbard bands [50]. When $U_d < \Delta$, the electronic structure corresponds to a Mott–Hubbard insulator, with the filled upper band being composed of the Cu*d*-type states. When $U_d > \Delta$, we have a charge-transfer insulator. In the latter case, the lower Hubbard band is situated below the oxygen subband, and a minimal electron excitation energy is required for the electron charge transfer to occur from the oxygen sublattice to copper centers.

Magnetism of individual copper atoms in undoped cuprates is simply and naturally explained in terms of the three-band Hubbard model. Indeed, when the copper *d* band is split into two Hubbard bands, corresponding to the $d^9 \longrightarrow d^8$ and $d^{10} \longrightarrow d^9$ excitations, the number of the remaining electrons per formula unit is even, which explains the insulating behavior of these compounds. Since the d^9 configuration corresponds to a magnetic ion, it is not surprising that magnetism occurs [51, 52].

The long-range antiferromagnetic order in such compounds is due to the spin superexchange between copper centers having one vacancy. It can be described by performing a unitary transformation that reduces the three-band model to the two-dimensional Heisenberg model [53]

$$H = J_{CC}\sum_{\langle i,j\rangle}(S_iS_j - 1/4n_i^d n_j^d),$$

where J_{CC} is the exchange coupling constant and S_i is the spin operator of a copper center. We have

$$J_{CC} = (4t_{pd}^4/\Delta)(1/U_d + 2/(2\Delta + U_p)).$$

A lower experimental estimate of this constant is $J_{CC} \cong 0.15$ eV.

Another evident success of Hubbard-type models in studying undoped high-T_c superconductors is the fact that, using this approach, it has been possible to qualitatively describe CuK_α X-ray spectra and Cu2*p* X-ray electron spectra (Cu2*p*-XPSs) of these compounds [52, 54–57]. However, in most of those papers, only the mechanisms of the formation of spectra for a one-hole configuration were discussed, ignoring the contribution from two-hole configurations, for which electron correlations are of fundamental importance.

For a two-hole configuration of the structural unit of a high-T_c superconductor, this problem was first solved by Zhang and Rice [58]. One would think that, in a charge-transfer insulator, an extra hole should be situated in the oxygen subband, which is just below the upper Hubbard band. However, Zhang and Rice argued against this point of view. They demonstrated that the covalent mixing of atomic states of copper and oxygen (due to which, in the band theory, the π band is basically of an oxygen nature, see Fig. 4) leads to the formation of a triplet and a singlet (Zhang–Rice singlet) in the Cu3d^9O2p^5 states through Hubbard splitting of occupied states in the one-electron π band. According to their calculations, the singlet is the highest of the occupied states (in the electron representation) and it is the first to be occupied by an extra vacancy produced in the process of doping.

In terms of the one-band Hubbard model, this means that both the Zhang–Rice singlet and the Cu3d^{10} vacuum state are nondegenerate and similar in behavior to the upper and lower Hubbard bands. Hence, they can be described in terms of an effective Hubbard model with a half-filled band,

$$H = -t\sum_{\langle i,j\rangle}^{nn}(c_{i\sigma}^+ c_{j\sigma} + \text{H.c.})$$
$$-t'\sum_{\langle i,j\rangle\sigma}^{nnn}(c_{i\sigma}^+ c_{j\sigma} + \text{H.c.}) + U\sum_i n_{i\uparrow}n_{i\downarrow},$$

where $n_{i\sigma} = c_{i\sigma}^+ c_{i\sigma}$ is the electron density for spin σ and $U \approx \Delta$. In addition to the hopping integral *t* between nearest neighbors (equal to 430 meV), this model involves the hopping integral on atoms of the next coordination shell ($t' = -70$ meV) [53].

In a CuO_4 cluster, the single oxygen state that is mixed with a copper *d* state is described by the totally symmetric combination $P_{B\sigma}^+ = (1/2)\sum_i p_{i\sigma}^+$. The other three oxygen states $P_{NB\alpha\sigma}^+$ are not binding states. In the half-filled state, the cluster has one vacancy with spin down. When one more hole is added (in the process of doping), we have the problem of two holes for four states interacting with the copper states.

Thus, we have the following five configurations (basis wave functions): the Cud^8O2p^6 configuration, represented by the state $|d_{j\uparrow}^+ d_{j\downarrow}^+\rangle$; the Cu$d^{10}$O2$p^4$ configuration, represented by $|P_{B\uparrow}^+ P_{B\downarrow}^+\rangle$; the Cu$d^9$O2$p^5$ configurations of the first type represented by the singlet $|S\rangle = (|P_{B\uparrow}^+ d_{j\downarrow}^+\rangle + |d_{j\uparrow}^+ P_{B\downarrow}^+\rangle)/\sqrt{2}$ and the triplet $|T\rangle = (|P_{B\uparrow}^+ d_{j\downarrow}^+\rangle - |d_{j\uparrow}^+ P_{B\downarrow}^+\rangle)/\sqrt{2}$. The Cu$d^9$O2$p^5$ configurations of the second type are represented by the states involving the nonbinding oxygen states, such as $|P_{NB\alpha\uparrow}^+ d_{j\downarrow}^+\rangle$.

The Hamiltonian of this model is not difficult to diagonalize. In the case of a charge-transfer insulator, the ground state is found to be the Zhang–Rice singlet, whereas the triplet is 2–4 eV higher and plays no part in the phenomenon in question at low temperatures. In this model, the Zhang–Rice singlet represents an effec-

tive spinless hole (in the doubly occupied-state subspace) moving through the two-dimensional spin lattice.

The other approach that allows one to consider strong electron correlations is multiconfiguration *ab initio* calculations (CI method and MC SCF approximation). For Cu(II) oxide systems, these calculations demonstrate strong localization of valence band top electrons (see, e.g., [59, 60]), which substantiates the applicability of Hubbard-type models. The most detailed study, in our opinion, was carried out in [60], where it was shown that the process of ionization of both core and valence orbitals is accompanied by a strong screening effect, which leads to the emergence of multielectron shakedown satellites in electronic spectra associated with the charge transfer from the occupied O2*p* to vacant Cu3*d*σ orbitals.

Of the papers in which the *ab initio* MC SCF method was used to investigate doped copper oxide [formally, Cu(III)] systems, of special note is that by Eto and Kamimura [61]. In that paper, the electronic structures of compounds La–Se–Cu–O and Nd–Ce–Cu–O were calculated by a multiconfiguration variational method in a cluster approximation. Calculations were performed for the CuO_6, CuO_4, Cu_2O_{11}, and Cu_2O_7 clusters. It was shown that, at the hole concentration close to the superconducting value, the ground state of the hole-doped CuO_6 cluster changes over from $^1A_{1g}$ to $^3B_{1g}$ when the copper–apical-oxygen internuclear distance is varied. The ground state of the electron-doped CuO_4 cluster was shown to be $^3B_{1g}$ and the dopant electron was at the Cu4*s* orbital. Eto and Kamimura also adequately described the antiferromagnetic ordering in the Cu_2O_{11} and Cu_2O_7 clusters and showed that doping suppresses antiferromagnetism in both *p*-type (Cu_2O_{11} cluster) and *n*-type (Cu_2O_7 cluster) systems, though the mechanisms of these processes are different.

1.6. A multielectron Model for the CuO_2 Plane

In a multielectron approach, the Hamiltonian of the multi-band *p–d* model, describing the valence state of copper and oxygen, can be written in the hole representation as [62–64]

$$H = H_d + H_p + H_{pp} + H_{pd},$$

$$H_d = \sum_r H_d(r),$$

$$H_d(r) = \sum_{\lambda\sigma}[(\varepsilon_{d\lambda} - \mu)d^+_{r\lambda\sigma}d_{r\lambda\sigma} + (1/2)U_d n^\sigma_{r\lambda}n^{-\sigma}_{r\lambda}]$$

$$+ \sum_{\sigma\sigma'}(V_d n^\sigma_{r1}n^{\sigma'}_{r2} - J_d d^+_{r1\sigma}d_{r1\sigma}d^+_{r2\sigma'}d_{r2\sigma}),$$

$$H_p = \sum_i H_p(i),$$

$$H_p(r) = \sum_{\alpha\sigma}[(\varepsilon_{p\alpha} - \mu)p^+_{i\alpha\sigma}p_{i\alpha\sigma} + (1/2)U_p n^\sigma_{i\alpha}n^{-\sigma}_{i\alpha}]$$

$$+ \sum_{\sigma\sigma'}(V_p n^{\sigma'}_{i1}n^{\sigma'}_{i2} - J_p p^+_{i1\sigma}p_{i1\sigma'}p^+_{i2\sigma'}p_{i2\sigma}),$$

$$H_{pd} = \sum_{i,r} H_{pd}(i, r),$$

$$H_{pd}(i, r) = \sum_{\lambda\alpha}\sum_{\sigma\sigma'}(T_{\lambda\alpha}p^+_{i\alpha\sigma}d_{r\lambda\sigma} + \text{H.c.}$$

$$+ V_{\lambda\alpha}n^\sigma_{r\lambda}n^{\sigma'}_{i\alpha} - J_{\lambda\alpha}d^+_{r\lambda\sigma}d_{r\lambda\sigma'}p^+_{i\alpha\sigma'}p_{i\alpha\sigma}),$$

$$H_{pp} = \sum_{(i,j)\alpha\beta\sigma}\sum(t_{\alpha\beta}p^+_{i\alpha\sigma}p_{j\beta\sigma} + \text{H.c.}), \qquad (1)$$

where $\varepsilon_{p\alpha}$ and $\varepsilon_{d\lambda}$ are the one-particle energies of *p*- and *d*-hole orbitals α and λ, respectively; U_p and U_d are the Hubbard correlation parameters; V_p and V_d are the matrix elements of the intraatomic Coulomb repulsion at the same and different orbitals of oxygen and copper; J_p and J_d are the Hund exchange integrals at oxygen and copper atoms, respectively; $T_{\lambda\alpha}$ and $t_{\lambda\alpha}$ are the matrix elements of *p–d* and *p–p* hopping, respectively, between their nearest neighbors; $V_{\lambda\alpha}$ and $J_{\lambda\alpha}$ are the matrix elements of the Coulomb and exchange interactions, respectively, between nearest copper–oxygen neighbors; and μ is the self-consistently calculated chemical potential, situated in the insulator energy gap of the undoped system. Obviously, the correctness of the results obtained in this model depends on the basis functions chosen for calculations. For this reason, one should include at least the $d_{x^2-y^2}$ and d_{z^2} orbitals of copper, as well as the p_x and p_y orbitals for all oxygen atoms. The energy of the $d_{x^2-y^2}$ orbital was taken to be ε_d, the energy of the d_{z^2} orbital was $(\varepsilon_d + \Delta_d)$, and the energy of the $p_{x,y}$ orbitals was ε_p.

In (1), the first two terms describe intraatomic interactions, including the Hubbard correlations U_p and U_d, the Coulomb interaction between holes at different orbitals and the Hund exchange. The last two terms in (1) correspond to interatomic *p–p* and *p–d* hopping and Coulomb interaction. The values of the parameters of the Hamiltonian (1) are taken from the experiment; they were determined by matching the electronic structure of the ground state of La_2CuO_4 to the optical and magnetic data [65]

$$V_p = 3 \text{ eV}, \quad V_d = 4.5 \text{ eV},$$

$$J_p = J_d = 0.5 \text{ eV},$$
$$T_{\lambda\alpha} = 1.5 \text{ eV}, \quad t_{\lambda\alpha} = 0.2 \text{ eV},$$
$$V_{\lambda\alpha} = 0.6 \text{ eV}, \quad J_{\lambda\alpha} = 0.2 \text{ eV},$$
$$\varepsilon_d = 0, \quad \Delta_d = 1.5 \text{ eV}, \quad \varepsilon_3 = 2 \text{ eV}.$$

The dependence of the results on the choice of U_p and U_d is discussed below. The parameters U_p and U_d are assumed to be infinite, unless otherwise specified.

1.7. The Ground State of the CuO_4 Cluster

Let us consider localized states with no hopping between unit cells. Figure 5 shows the local bases for (a) the Hubbard model and (b) a multi-band *p–d* model; in the latter case, only several excited states with $n = 1$ and $n = 2$ [65, 66] are shown for a particular unit cell in which a quasiparticle is created. In the hole representation of the Hubbard model (Fig. 5a), the top of the valence band consists only of two quasiparticles [67] (in terms of the multielectron approach), corresponding to the upper and lower Hubbard bands with energies

$$\Omega_+ = E_0(2, S) - E_0(1) = E_0(1) + U$$

and

$$\Omega_- = E_0(1) - E_0(0) = E_0(1),$$

where $E_0(0)$, $E_0(1)$, and $E_0(2, S)$ are the energies of the ground states of the cluster in the zero-, one-, and two-particle subspaces of the Hilbert space. The $S = 1/2$ state with the energy $E_0(1)$ is degenerate due to spin, whereas the state with $E_0(2, S)$ may be a singlet ($S = 0$) or a triplet ($S = 1$). Dispersion in the system [$\Omega_S \longrightarrow \Omega_S(k)$] is associated with intercluster hopping. The dispersion relation varies with different values of S; hence, the X-ray spectra will be different for systems differing in spin.

In a many-band model, the number of different transitions between states in which the numbers of electrons (or holes) differ by unity is much larger (Fig. 5b). It is much more convenient to describe the localized particles, introduced in these models, in terms of the Hubbard operators

$$X^{pq} = |p\rangle\langle q|,$$

which are constructed for a complete set of localized multielectron states. Here, as indicated above, the states of one unit cell, that is, multielectron molecular orbitals, are implied.

In terms of the three-band *p–d* model, in the case where $T_{\lambda\alpha} \ll \Delta$, U_p, U_d ($T_{\lambda\alpha}$ is the *p–d* hopping parameter and $\Delta = \varepsilon_d - \varepsilon_p$ is the charge-transfer energy), the effective exchange integral $J_{\text{Cu–O}}$ can be written as [53]

$$J_{\text{Cu–O}} = 8T_{\lambda\alpha}^2(1/(\Delta + U_p) + 1/(D_d - \Delta)).$$

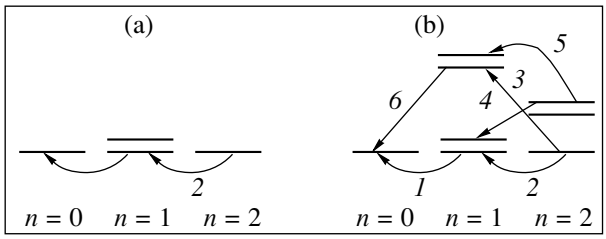

Fig. 5. Local bases of (a) the one-band Hubbard model and (b) the multiband *p–d* model. Only some of the excited terms are shown in the one-hole and two-hole subspaces of the Hilbert space in the multiband model. Arrows show the processes of quasiparticle annihilation.

In the limit of $U_p = U_d = \infty$, the exchange integral $J_{\text{Cu–O}}$ is zero and the singlet and triplet are degenerate. However, at finite U_p and U_d, the value of $J_{\text{Cu–O}}$ becomes large; for typical values of parameters $U_d = 10$ eV, $U_p = 6$ eV, $T_{\lambda\alpha} = 1$–1.5 eV, and $\Delta = 2$–3 eV, we have $J_{\text{Cu–O}} = 2$ eV. Therefore, in order to correctly evaluate the effective exchange integral, one should take into account the finiteness of the intraatomic Coulomb repulsion parameters U_p and U_d.

The state of two holes in the CuO_4 unit cell may be a Zhang–Rice singlet [58] or a triplet [68]. When calculating the spectra, the energies of the singlet (ε_S) and the triplet (ε_T) were determined by exactly diagonalizing the Hamiltonian of the CuO_4 cluster at $U_p = U_d = \infty$. Relatively small variations in the values of parameters may result in the crossover between the singlet and triplet, that is, in the change of sign of the level splitting $\Delta\varepsilon = \varepsilon_T - \varepsilon_S$. In our case, at $\Delta = \varepsilon_p - \varepsilon_d = 2$ eV, the ground state of two holes is a triplet ($\varepsilon_T = -0.93$ and $\varepsilon_S = -0.82$), while at $\Delta = 1.5$ eV, the ground state is a singlet ($\varepsilon_T = -1.52$ and $\varepsilon_S = -1.54$).

When the values of the Hubbard repulsion parameters are finite, the picture becomes somewhat different. Figure 6 shows calculated level splitting [69] in the multiband *p–d* model for $U_d = 12$ eV, $U_p = 8$ eV, $T_{\lambda\alpha} = 1.5$ eV, and $\Delta = 3$ eV (curve *1*). This curve corresponds to a minimal set of parameters, which is arbitrarily called "three-band model plus d_{z^2} orbital," because all parameters that are not involved in the three-band model are taken to be zero. The calculations for this set explicitly show the effect of the d_{z^2} orbital when its energy is lowered to its actual values.

As Δ_d is decreased, the effect of the Coulomb interaction between orbitals increases, as seen from curve *2*, for which we have taken $V_d = 4.5$ eV. Curve *3* corresponds to the case where all the parameters we used to completely calculate the CuO_2 layer are taken to be nonzero.

It is seen from Fig. 6 that the exchange splitting $\Delta\varepsilon$ decreases as the energies of the $d_{x^2-y^2}$ and d_{z^2} orbitals

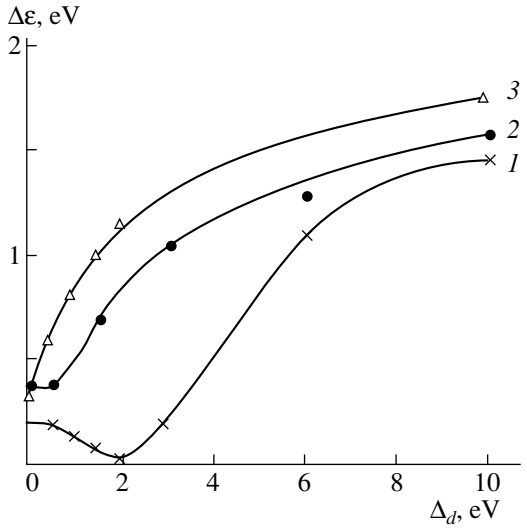

Fig. 6. Dependence of the triplet–singlet splitting energy $\Delta\varepsilon = \varepsilon_T - \varepsilon_S$ for the two-hole states of the CuO_4 cluster on the crystal-field parameter $\Delta_d = \varepsilon d_{z^2} - \varepsilon d_{x^2-y^2}$. The model parameters are (eV): (*1*) $U_d = 12$, $U_p = 8$, $\Delta = 3$, $T_{\lambda\alpha} = 1.5$, and other parameters are zero; (*2*) $V_d = 4.5$ and the other parameters as for curve *1*; and (*3*) $U_d = 12$, $U_p = 8$, $\Delta = 2$, $T_{\lambda\alpha} = 1.5$, $t_{\alpha\beta} = 0.2$, $V_d = 4.5$, $V_p = 3$, $V_{pd} = 0.6$, $J_p = J_d = 0.5$, and $J_{pd} = 0.2$.

approach each other. Virtual transitions to orbitally nondegenerate states lead to antiferromagnetic exchange and stabilize the singlet, whereas virtual transitions to degenerate states lead to ferromagnetic exchange and stabilize the triplet. The latter is due to the fact that, according to the Stoner criterion, the density of states at the Fermi surface increases in proportion to the degeneracy.

Thus, the transition from the three-band to the multiband *p–d* model with finite values of the Hubbard correlation parameters leads to a decrease in $\Delta\varepsilon$, from 2–4 eV in the former case to 0.1 eV in the latter. The introduction of other small parameters into the many-band model may lead to the inversion of the singlet and triplet states. For instance, these may be oxygen–oxygen hopping parameters $t_{\lambda\alpha}$ [68], interatomic Coulomb and exchange *p–d* integrals V_{pd} and J_{pd}, or the contribution from apical oxygen atoms.

1.8. General Characterization of the Electronic Structure of the HTSC Oxides

Thus, on the basis of the data obtained by various experimental and theoretical methods and presented above, the following current view of the electronic structure of high-T_c superconductors was formed [53].

The Hubbard repulsion removes the degeneracy of the upper half-filled one-electron band σ^* (Figs. 4, 7a), splitting it into the lower and upper Hubbard bands (LHB and UHB, respectively) depending on the relative values of the parameters t_{pp}, t_{pd}, U_d, and Δ (Figs. 7b, 7c). According to the classification by Zaanen, Sawatzky, and Allen [50], there are three types of electronic structures (Fig. 7): (a) *d*-type metal, corresponding to $U_d = 0$ (this case was discussed in Subsection 1.4); (b) the Mott–Hubbard insulator, where t_{pp}, t_{pd} <

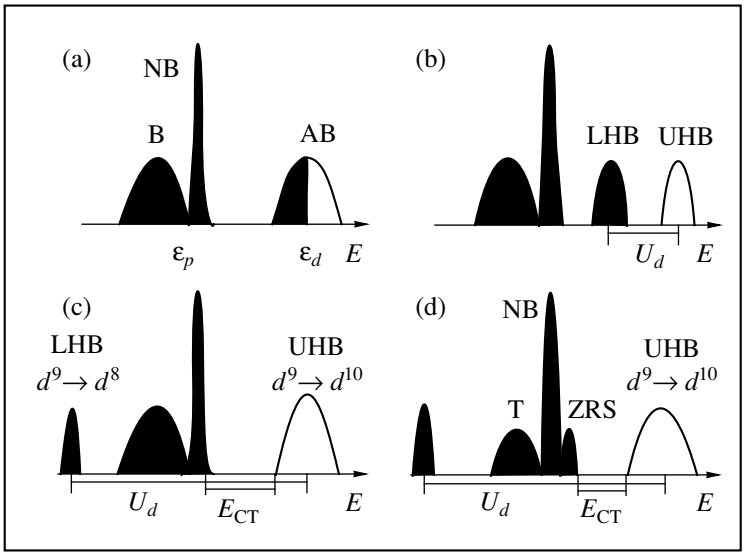

Fig. 7. (a–c) Zaanen–Sawatzky–Allen classification [50] of the one-particle spectra of transition-metal compounds: (a) metal, (b) Mott–Hubbard insulator, and (c) charge-transfer insulator (CTI); and (d) CTI with Zhang–Rice singlet–triplet splitting. Shaded regions indicate occupied states, (N)[A]B are (non)[anti]bonding states, L(U)HB are lower (upper) Hubbard bands, ZRS is the Zhang–Rice singlet, T is the triplet, E_{CT} is the renormalized charge-transfer gap, and *E* is the energy.

$U_d \ll \Delta$ and (c) the charge-transfer insulator, where t_{pp}, $t_{pd} < \Delta < U_d$.

The experimental resonance photoelectron spectroscopy data, which allow one to determine the partial contributions from the O2*p* and Cu3*d* states, suggest that the electronic structure of high-T_c superconductors corresponds to a charge-transfer insulator. Measurements showed [70–72] that, in the $La_{2-x}Sr_xCuO_4$, $YBa_2Cu_3O_{7-\delta}$, and $Nd_{2-x}Ce_xCuO_4$ compounds, the parameter U_d of the three-band Hubbard model is much larger than Δ. It was found, while making a comparison of the experimental data and cluster calculations [70–72], that U_d ranged in magnitude from 7.3 to 10.5 eV.

In the one-electron π subsystem, the Hubbard repulsion manifests itself in the same way, splitting it into a triplet and a singlet state. According to [58], among the occupied states in undoped high-T_c superconductors, the singlet has the highest energy and, in terms of the Hubbard model, it is an analog of the UHB, whereas the triplet has a lower energy and corresponds to the LHB.

This last case of the electronic structure calculated for the undoped superconductors in the Hubbard model is shown in Fig. 7d. The ZRS peak corresponds to the Zhang–Rice singlet, which is the ground state among the two-hole states [58].

2. A SUDDEN-PERTURBATION (SP) MODEL AND A SCHEME FOR CALCULATING SPECTRAL CHARACTERISTICS

2.1. The Theoretical Fundamentals of X-ray Spectroscopy (Sudden-Perturbation Model)

The formation of X-ray (absorption and emission) spectra and of X-ray electron spectra is associated with a one-electron and a one-photon process; that is, the electronic system interacts with one X-ray quantum, and one electron makes a transition from some core or valence orbital to a highly excited state. Other (say, Auger) processes that accompany or follow this process noticeably differ in transition energy (which allows one to resolve them) and, in addition, the particles emitted or absorbed in them differ in nature. The processes of the interaction of X-rays with the matter we consider here obey the energy conservation law, and all channels of excitation and decay of highly excited states in these processes are known.

Since the early 1930s, the theory of the interaction of X-rays with matter has been based on the sudden-perturbation (SP) approximation, which was successfully employed to treat the processes in the electron shell of an atom that accompany the α, β^-, and β^+ decay of nuclei, *K*-capture, and multiple ionization of atoms [73–77]. Later, this approximation was extended to all cases of inelastic interaction of X-rays with matter.

The SP model is based on the assumption that, due to some interaction, the Hamiltonian of the system is suddenly changed [78, 79] as compared with the overall duration of the corresponding process or the lifetime of the system. This is true in the case of *K*-capture or β decay. Indeed, the lifetime of the excited state of the electronic system with a vacancy at the 1*s* orbital (from which an electron has fallen on the nucleus), as evaluated from the experimental X-ray line widths ($\Delta E = \Gamma \approx 1$ eV) and the Heisenberg uncertainty relation, is of the order of $\tau^* = \Delta t > \hbar/\Delta E \approx 10^{-15}$ s. At the same time, the time τ_K it takes for the electron to "fall" on the nucleus can be estimated as the ratio of the effective orbit radius R_{1s} (~0.1 au) to the effective velocity ν_{1s} of an electron moving in this orbit. The latter can be evaluated from the virial theorem (the kinetic electron energy is obtained to be about 10^3–10^4 eV) and, hence, the time τ_K is of the order of ~10^{-19}–10^{-18} s, which is far shorter than the lifetime (10^{-15} s) of the ionized excited state of the atom with the charge of its nucleus changed by unity. Thus, in the case of the *K*-capture, one can assume that the Hamiltonian of the system suddenly changes in comparison with the lifetime of the final highly excited state with an electron vacancy at the 1*s* orbital. In the case of the β decay, the change in the charge of the nucleus occurs even more quickly, because the radius of the atomic nucleus is much smaller than that of the electron shells.

The applicability of the SP model is also well founded for the X-ray spectroscopy of inner shells. For example, it can be used to describe K_α spectra, which are associated with transitions from 2*p* states to the ionized 1*s* state (the transition energy is of the order of 10^4 eV for elements in the middle of the periodic system). Such spectra are commonly measured for excitation energies 3–5 times higher than the *K*-shell energy E_K, because in this case the line strength ceases to depend on the excitation energy, which is due to the nature of vacant states with energies of the order of 10^4 eV (above the ionization threshold). Hence, one can take the energy of an exciting photon to be $\hbar\bar{\omega} \gg E_K$. In the SP model, it is assumed that an 1*s* electron is so quickly removed that the potential for 2*p* electrons changes suddenly. Hence, the time it takes for the 1*s* electron to go out of the *L* shell should be small in comparison with the revolution period of 2*p* electrons,

$$r_{2p}/\nu_{1s} \ll 2\pi r_{2p}/\nu_{2p},$$

here, r_{2p} is the orbit radius of 2*p* electrons (0.25 au for copper). Taking the excitation energy to be ~10^4–10^5 eV and using the virial theorem, one obtains $\nu_{1s} \sim 3 \times 10^9$–$10^{10}$ cm/s and $\nu_{2p} \sim 5 \times 10^7$–$10^8$ cm/s for elements in the middle of the periodic table. Thus, the condition for suddenness is fulfilled and mixing of the 1*s* electron with the 2*p* shell does not occur.

However, a more detailed consideration of the formation of even these high-energy X-ray spectra, associated with inner shells, raises some questions. Undoubtedly, the effective nucleus charge, as it does for the 2*p* shell, Z_{2p}, changes suddenly, but the 2*p* shell

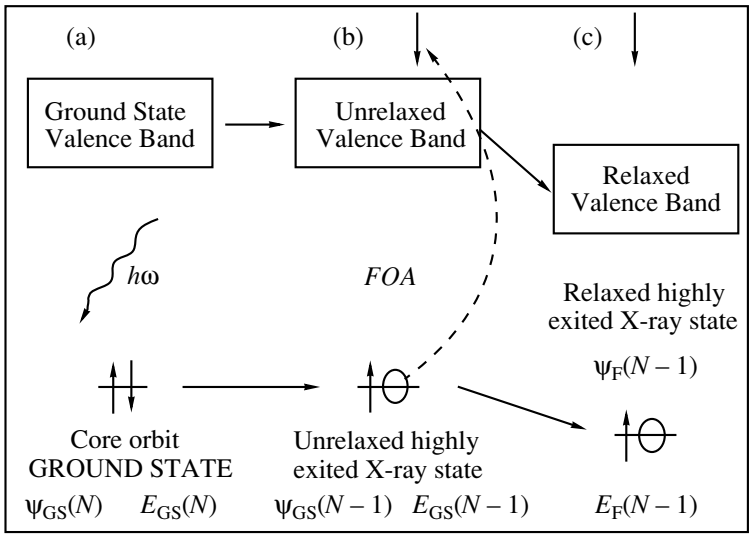

Fig. 8. Process of excitation of the electron system by an X-ray quantum (schematic): (a) the ground state of the system before absorption of an X-ray quantum $\hbar\omega$; (b) the final state of the electron system in the frozen-orbital approximation (*FOA*), described by the wave function Ψ_0^* and energy E_0^*, with a hole at the core energy level, a photoelectron in the continuum, and with the unrelaxed valence band; and (c) the final quasi-stationary state of the relaxed electron system with the X-ray hole, described by the wave function Ψ^* and energy E^*.

itself will be affected by the electron going through and out of the electron system (a distance of roughly 2 au). This increases the duration of the system perturbation by at least an order of magnitude (up to 10^{-17}–10^{-18} s) and becomes comparable to the revolution period of $2p$ electrons (about 10^{-17} s). Furthermore, considering this process formally, we should add a time-dependent perturbation term to the initial Hamiltonian of the system.[1] Therefore, in terms of quantum mechanics, the energy is not conserved in this process.

It is here that a hidden paradox arises when one discusses the applicability of the SP model in the context of X-ray spectroscopy theory. On the one hand, the process of the electron going out of the system causes a perturbation finite in time, which must lead to the violation of the energy conservation. On the other hand, no other particles (quanta or electrons) are emitted or absorbed, and they are not involved directly in the formation or decay of highly excited states; hence, energy must be strictly conserved.

For the valence shell, the revolution period of electrons, as evaluated from the effective radius ($R_{vs} \approx 3$ au) and their energy ($E_{vs} \approx 5$ eV), is of the order of 5×10^{-16} s, which is close to the lifetime (10^{-15} s) of a highly excited state. Hence, the valence electrons have no time to make a sufficient number of revolutions about the nucleus during the lifetime of the excited state. Due to this fact, it is commonly assumed in X-ray spectroscopy [80] that the transition of an electron system, induced by an X-ray quantum, from the ground state with a wave function $\Psi_{GS}(N)$ and an energy $E_{GS}(N)$ to a final quasi-stationary highly excited state with an X-ray hole at a core orbital [with a wave function $\Psi_F(N-1)$ and an energy $E_F(N-1)$], proceeds via a transient, "unrelaxed," highly excited state $\Psi_{GS}(N-1)$ with an energy of $E_{GS}(N-1)$. In this transient state, the hole is already created at a core orbital, but the other part of the electron system has not yet adapted itself to it (has not relaxed, in terms of X-ray spectroscopy, see Fig. 8). In this scheme, it is assumed that the rearrangement time of the valence shell τ_r is longer than the duration of the perturbation or, what is the same, longer than the time it takes for the electron to leave the core, $\tau_c = a/v \approx a/\sqrt{2\hbar\bar{\omega}/m_e}$, where a is the effective distance the electron travels before it leaves the system (which is roughly 2–3 au), v is the velocity of the electron at which it goes out of the system, and $\hbar\bar{\omega}$ is the energy of the absorbed quantum.

The currently available methods for studying matter that are based on the excitation by X-rays are used, first of all, to investigate the valence shell of the electron structure, the effective radius of which is 2–5 au. In these methods (X-ray absorption spectroscopy, X-ray emission spectroscopy, and some other techniques, by which the specified channels of the creation and decay of highly excited X-ray states are investigated), significantly lower excitation energies are used, 10^3–10^2 eV, which are often close to the ionization thresholds of

[1] In fact, the photoelectron no longer belongs to the system in question and, hence, its exit from the system affects the latter, giving rise to a time-dependent perturbation or, in terms of X-ray spectroscopy, to the time-dependent process of "relaxation" of the electron energy levels.

core states. Let us evaluate the time it takes for an electron to leave the system and travel a distance (about 10 au) at which the photoelectron no longer affects the electronic structure of the X-ray cation. We will take the energy E_i of the core state from which an electron is knocked to be 1000 eV (2*p* state of copper) and the energy of exciting radiation $\hbar\bar{\omega}$ to be equal to the ionization threshold (also 1000 eV).

For the core state before the absorption of an X-ray quantum, the virial theorem holds; hence, $E_i = T_i + V$ and $E_i = -T_i$. Immediately after the absorption (the initial instant), the potential energy of the system is not changed (because the nucleus charge and the electron charge distribution remain the same), but the total energy of the electron at the initial instant $E_f(t = 0)$ becomes equal to $(E_i + \hbar\bar{\omega})$. Under these conditions, the kinetic energy of the photoelectron at the initial instant is $T_f(t = 0) = -2E_i$ and at the infinitely long time $t \longrightarrow \infty$, it is equal to zero. Therefore, we can evaluate the effective velocity of the photoelectron; it is obtained as $(\nu_p(t_0) = 2.5 \times 10^8$ cm/s at the initial instant and $\nu_p(t_\infty) = 0$ at the final instant. Accordingly, the average velocity is 10^8 cm/s, whereas the time it takes for the photoelectron to move a distance of 10 au (5×10^{-8} cm) is $\tau_p = 5 \times 10^{-16}$ s.

At the present time, X-ray methods are being developed in which the effective time it takes for an electron to leave the system can be longer by several orders of magnitude than the estimate made above. For example, in X-ray absorption spectroscopy, the case is rather common where many-center scattering of a photoelectron occurs by nearest-neighbor atoms (XANES range of X-ray absorption spectra); or a photoelectron resides near the absorbing atom for an anomalously long time, because around this atom there is a high positive barrier due to vacant electron states with a large *l* (giant-resonance spectra in lanthanides and actinides); or a photoelectron, being several atomic units away from the positively charged X-ray hole, is attracted to it (X-ray excitons).

Thus, it is seen that the lifetime of highly excited X-ray states and the time it takes for a photoelectron to leave the system, as well as the revolution period of valence shell electrons, are of the same order of magnitude in the case of the formation of spectra associated with the structure of valence states.

In spite of this, the SP model adequately describes X-ray processes of various types. In the process of absorption of an X-ray quantum, the total energy of the system is changed by the quantum energy $\hbar\bar{\omega}$ and the final energy of the highly excited state is $E_f = (E_i + \hbar\bar{\omega}) =$ const. Thus, it is seen that the energy conservation law is strictly obeyed in the process of interaction of X-ray quanta with matter.

Taking into account that $E_f = (E_i + \hbar\bar{\omega}) =$ const, we can write the wave function of the final state in the form

$$\Psi_F^n(x, t) = \exp\left(-\frac{i}{\hbar}E_F^n t\right)\Phi_F^n(x),$$

which is a solution to the time-dependent Schrödinger equation

$$i\hbar\frac{\partial\Psi_F^n(x, t)}{\partial t} = H\exp\left(-\frac{i}{\hbar}E_F^n t\right)\Phi_F^n(x),$$

where *H* is the Hamiltonian of the system. Analogously, the initial (ground) state of the system can be written as

$$\Psi_{GS}(x, t) = \exp\left(-\frac{i}{\hbar}E_{GS} t\right)\Phi_{GS}(x).$$

According to quantum mechanics, the probability of the dipole transition from the initial to the final state is given by the formula

$$I_F^n(x, t)$$

$$\approx \left|\int \exp\left(\frac{i}{\hbar}E_{GS} t\right)\Phi_{GS}^*(x) r \exp\left(-\frac{i}{\hbar}E_F^n t\right)\Phi_F^n(x) dx\right|^2$$

$$= \left|\left(\exp\left(\frac{i}{\hbar}E_{GS} t\right)\exp\left(-\frac{i}{\hbar}E_F^n t\right)\right)\int \Phi_{GS}^*(x) r \Phi_F^n(x) dx\right|^2.$$

The total energies of the initial and final states are very large; for individual atoms and molecules, we have $E_{GS} \approx E_F^n \approx 10^4$–$10^5$ eV, while for a solid, in which the effective volume in which the interaction of an electromagnetic quantum with matter takes place may comprise as many as 10 atoms, we have $E_{GS} \approx E_F^n \approx 10^5$–$10^6$ eV. At the initial instant, the time-dependent factors in both the initial and final states are equal to unity and, in addition, the continuity condition for the wave function is fulfilled

$$\exp\left(-\frac{i}{\hbar}E_{GS} t_{(t=0)}\right)\Phi_{GS}(x) = \exp\left(-\frac{i}{\hbar}E_F^n t_{(t=0)}\right)\Phi_F^n(x),$$

$$\Phi_{GS}(x)_{(t=0)} \equiv \Phi_F^n(x)_{(t=0)}.$$

Therefore, for the probability of dipole transitions, we have a conventional formula

$$I_F^n(x) = \left|\int \Phi_{GS}^*(x) r \Phi_F^n(x) dx\right|^2.$$

Thus, the only process that is associated with the formation of X-ray spectra and proceeds "in a moment" is the interaction of the X-ray quantum with a core electron. Therefore, in the SP model, the Hamiltonian of the system in a highly excited X-ray state can be written as

$$H_{ex} = H_0 + H_{c,d}, \quad (2)$$

where H_0 is the Hamiltonian of the unperturbed system (1) and $H_{c,d}$ is the term describing the interaction of a core hole with the other part of the electron system,

$$H_{c,d} = V_{c,h}\sum d^{+}_{r\lambda\sigma}d_{r\lambda\sigma}n_c,$$

where $n_c = \sum_\sigma n_{c\sigma}$ is the number operator of X-ray-produced vacancies at a core orbital.

It follows from the above consideration that the state with $\Psi_{GS}(N-1)$ and $E_{GS}(N-1)$ does not occur; instead, an X-ray quantum induces the transition of the system from the stationary ground state (Ψ_{GS}, E_{GS}) to the final (for the process in question) quasi-stationary state (Φ_F, E_F) with the lifetime τ^* via the transient state $[\Phi_T(N, t)E_T(N, t)]$, the lifetime of which is equal to τ_c (the time it takes for the core electron to leave the system); hence, the duration of the rearrangement of the electron system is $\tau_r = \tau_c$. The change in energy of the electron shells in the process of relaxation associated with the X-ray-created hole is of the order of 1–10 eV, whereas the total excitation energy of the system is $\hbar\bar{\omega} \sim 1000$ eV; that is, the change in energy associated with the relaxation of the valence shell during X-ray processes is a small perturbation of the system.

2.2. The Influence of Strong Electron Correlations on the Spectrum Structure

When studying the X-ray and electron spectra of copper oxide high-T_c superconductors, one should take multielectron states into account, because the core hole strongly interacts with Cu3*d* electrons. Let us consider the absorption spectrum in the case where an inner-shell 1*s* or 2*p* hole is created. In one-electron calculations, the SP approximation in this case is better known as the Larson model [81–84]. The interaction of vacant electron states with X-ray-produced core 2*p* and 1*s* vacancies is described by the Coulomb matrix elements $V^p_{c,d} = 7.5$ eV and $V^s_{c,d} = 7$ eV, respectively.

It should be noted that, in the formation of X-ray absorption spectra, the final states may have no holes at copper atoms (transitions $2p \longrightarrow d^{10}$, $d^{10}\underline{L}$, $d^{10}\underline{L}\,s(\varepsilon)$, $d^{10}\underline{\underline{LL}}\,s(\varepsilon)$ and $1s \longrightarrow d^{10}\underline{L}$, $d^{10}\underline{\underline{LL}}$), one hole (transitions $2p \longrightarrow d^9 s(\varepsilon)$, $d^9\underline{L}\,s(\varepsilon)$, d^9 and $1s \longrightarrow d^9$, $d^9\underline{L}$), or two holes at copper atoms (transitions $2p \longrightarrow d^8 s(\varepsilon)$ and $1s \longrightarrow d^8$).

Before the creation of a hole at a core orbital of copper, the multielectron wave function of the system can be written as

$$\psi_{in} = \varphi_c^n \psi^{(pd)}_{in,0}, \tag{3}$$

where φ_c^n is the wave function of the core electron, *n* is the occupation number of the core orbital, and $\psi^{(pd)}_{in,0}$ is the wave function of the ground state of the valence electron system of copper and oxygen with the energy $E^{(pd)}_{in,0}$, described by the Hamiltonian (1) under the condition $n_d + n_p = n_h = \text{const}$, where n_d and n_p are the concentrations of holes in *d* states of copper and *p* states of oxygen, respectively, and n_h is the number of holes in a unit cell, being equal to 1 or 2, depending on the doping.

The wave function of the system in the final state with the unchanged number of vacancies in the valence shell (excluding the process of formation of the white line of the CuL_3 spectrum, in which the number of Cu3*d* vacancies is decreased by unity) and with one photoelectron in the *s*, *p*, or *d* continuum far beyond the ionization threshold can be written in the form

$$\Psi_f^{(m)} = \varphi_c^{n-1}\varphi_l\psi^{(pd)}_{f,m}, \tag{4}$$

where φ_l is the wave function of the photoelectron in the *l* state with an energy ε_l, to which this electron makes a transition after excitation, and $\psi^{(pd)}_{f,m}$ is the wave function of the *m*th term of the system of *p* and *d* electrons in the final state with the energy $E^{(pd)}_{f,m}$. The index *m* enumerates all eigenstates of the Hamiltonian $(1 + 2)H + H_{c,d}$ [given by (1) and (2)] that have a vacancy at a core orbital.

The energies of the initial and final states are

$$\begin{aligned} E_{in} &= n\varepsilon_c + E^{(pd)}_{in,0}, \\ E_{f,m} &= (n-1)\varepsilon_c + \varepsilon_l + E^{(pd)}_{f,m}, \end{aligned} \tag{5}$$

respectively, where $E^{(pd)}_{f,m}$ is the energy of the *m*th term of the final highly excited state. In the approximation where strong electron correlations and the formation of the white line of the CuL_3 spectrum are ignored, the energy of the absorbed X-ray quantum equals

$$\hbar\omega_0 = \varepsilon_l - \varepsilon_c. \tag{6}$$

When strong electron correlations are taken into account, the energy of the absorbed X-ray quantum is

$$\begin{aligned} \hbar\omega &= \varepsilon_l - \varepsilon_c + \Delta E_m, \\ \Delta E_m &= E^{(pd)}_{f,m} - E^{(pd)}_{in,0}. \end{aligned} \tag{6a}$$

Thus, in the one-electron approximation, we can write the energy of this quantum as $\hbar\omega_0 = \hbar\omega - \Delta E_m$.

X-ray absorption is described by the Hamiltonian

$$H_{X\text{-ray}} = \sum_k I^{(0,k)} c^{+} l_k,$$

where $I^{(0,k)} = |\langle\varphi_c|\mathbf{er}|\varphi_k\rangle|^2$ is the one-electron dipole matrix element, c^+ is the creation operator of a hole at a core orbital, and l_k is the annihilation operator of a hole in the valence shell or in the continuum. In the case

where the number of *d* holes remains unchanged (transitions to *s* or *p* orbitals), the intensity of an X-ray-induced transition is

$$I_m(\hbar\omega) = \left|\langle\varphi_{\text{in}}|\mathbf{er}|\psi_f^{(m)}\rangle\right|^2 = \left|\langle\varphi_c(\varepsilon_c)|\mathbf{er}|\varphi_l(\varepsilon_l)\rangle\right|^2 \times \left|\langle\psi_{\text{in},0}^{(pd)}(E_{\text{in},0}^{(pd)})|\psi_{f,m}^{(pd)}(E_{f,m}^{(pd)})\rangle\right|^2. \quad (7)$$

In the absence of strong Coulomb interaction between the hole at an inner-shell orbital and valence vacancies ($V_{c,d} = 0$), the functions $\psi_{\text{in},0}^{(pd)}(E_{\text{in},0}^{(pd)})$ and $\psi_{f,m}^{(pd)}(E_{f,m}^{(pd)})$ are mutually orthogonal and, hence, the last factor in (7), $I^{(c,m)}(\Delta E_m) = |\langle\psi_{\text{in},0}^{(pd)}(E_{\text{in},0}^{(pd)})|\psi_{f,m}^{(pd)}(E_{f,m}^{(pd)})\rangle|^2$, is equal to $\delta_{m,0}$. In this case, the transition probability is determined only by the matrix element $I^{(0,l)}(\hbar\omega_0) = \langle\varphi_c(\varepsilon_c)|\mathbf{er}|\varphi_l(\varepsilon_l)\rangle$, which is calculated in the one-electron approximation.

If the Coulomb interaction (2) is not ignored, the states of valence *p* and *d* electrons (holes) before and after photoionization cease to be orthogonal and, therefore, both the ground term and various excited terms of the final state contribute to the absorption spectrum.

The formation of the white line of the Cu$L_{2,3}$ spectrum is more difficult to analyze, because the number of holes in the *d* shell decreases. The wave function in this process can be written in the form

$$\Psi_f^{(m)} = \varphi_c^{n-1}\psi_{f,m}^{(pd)}(n_h - 1), \quad (8)$$

where $\psi_{f,m}^{(pd)}(n_h - 1)$ is the multielectron function in the $(n_h - 1)$-particle subspace of the Hilbert space. The energy of the final state is equal to

$$E_{f,m} = (n-1)\varepsilon_c + E_{f,m}^{(pd)}(n_h - 1) \quad (9)$$

while the energy of the absorbed X-ray quantum is

$$\hbar\omega = -\varepsilon_c + \Delta E_m. \quad (10)$$

The one-electron energies ε_d of the *d* orbitals of the initial and final states are included in the multielectron energies $E_{\text{in},0}^{(pd)}$ and $E_{f,m}^{(pd)}$; their values, as obtained by X_α calculations and used in treating the processes of this type, are roughly –2 to –3 eV.

In the absence of the strong Coulomb interaction with the X-ray hole (and, hence, in the absence of the relaxation of the electron system associated with the creation of this hole), the energies of the initial and final states of the *d* shells can be written as $E_{\text{in}}^0 = n\varepsilon_c + (10 - n_h)\varepsilon_d$ and $E_f^0 = (n-1)\varepsilon_c + (10 - n_h + 1)\varepsilon_d$, respectively. In this case, the one-electron transition energy is

$$E_f^0 - E_{\text{in}}^0 = \hbar\omega_0 = \varepsilon_d - \varepsilon_c$$

and, in addition,

$$\hbar\omega_0 = \hbar\omega - \Delta E_m.$$

Therefore, the intensity of the white line (associated with a decrease of the number of *d* holes by unity) can be written in the form

$$I_m(\hbar\omega) = \left|\langle\psi_{\text{in}}|\mathbf{er}|\psi_f^{(m)}\rangle\right|^2 = \left|\langle\varphi_c(\varepsilon_c)|\mathbf{er}|\varphi_d(\varepsilon_d)\rangle\right|^2 \times \left|\langle\psi_{\text{in},0}^{(pd)}(E_{\text{in},0}^{(pd)})|d_{r\lambda\sigma}|\psi_{f,m}^{(pd)}(E_{f,m}^{(pd)}, n_h - 1)\rangle\right|^2. \quad (11)$$

As in (7), we designate the one-electron contribution as $I^{(c,m)}(\Delta E_m)$ and the multielectron one as $I^{(0,l)}(\hbar\omega_0)$.

Summing (7) and (11) over multielectron transitions, we obtain an expression describing the whole spectrum,

$$I(\hbar\omega) = \sum_m I_m(\hbar\omega) = \sum_m I^{(0,l)}(\hbar\omega - \Delta E_m) I^{(c,m)}(\Delta E_m). \quad (12)$$

Thus, the total absorption spectrum $I(\hbar\omega)$ consists of a set of one-electron spectra, the intensity of the principal line of which is proportional to the multielectron factor $I^{(c,m)}(\Delta E_m)$ with $m = 0$, given by (7) and (11), and satellites, separated from the principal line by $\Delta E_m = E_{f,m}^{(pd)} - E_{\text{in},0}^{(pd)}$ and having an intensity determined by multielectron factors (7) and (11) with $m \neq 0$. As is seen, the X-ray absorption spectrum of the strongly correlated electron system is the discrete convolution of two spectra: the discrete spectrum $I^{(c,m)}(\Delta E_m)$ of transitions between *p* and *d* states of electrons (holes) and the one-electron spectrum $I^{(0,l)}(\hbar\omega - \Delta E_m^{(h)})$ of transitions from 1*s* and 2*p* core orbitals to vacant electron states situated both below and above the ionization threshold.

2.3. A One-Electron Model for Calculating X-ray Absorption Spectra

The problem of choosing a cluster for calculating the one-electron structure and spectra of high-T_c superconductors has long been solved [27]. The one-electron profiles of X-ray absorption spectra both below and above the ionization threshold were calculated in the self-consistent-field approximation for X_α scattered waves (SCF X_αSW) [85]. By now, the range of applicability of this approximation is well known. In this paper, the electronic structure of clusters CuO_6^{10-} and CuO_6^{9-} ($La_{2-x}Sr_xCuO_4$), corresponding to the (+2) and (+3) formal copper states, was calculated employing the X_α-OMEGA program complex [86], while the calculations of the electronic wave functions and one-electron X-ray dipole transition intensities in all energy range were performed using the X_α-CONTINUOUS program [87]. The cluster parameters were chosen

in accord with the internuclear spacing presented in [88, 89].

2.4. The Structure of the Final Spectra

The final spectra include both the effects of the density of vacant one-electron states and the doping of the $La_{2-x}Sr_xCuO_4$ compound and the effects of strong correlations in doped and undoped unit cells. These spectra are obtained by summing the one-electron spectra in accordance with (12). The *xy*-polarized CuL_3 spectrum of undoped La_2CuO_4 represents the (only possible) one-electron transition from the Cud^9 to the Cud^{10} configuration with an intensity of 0.3428 and an energy of 2.03 eV; the profile of the spectral line is obtained using the calculated profiles of one-electron spectral lines of the CuO_6^{10-} cluster by the SCF-X_αSW method. The polarized spectra of unit cells with two vacancies in the triplet ground state are more complex; for instance, the *xy* component is formed by transitions from the ground two-hole state to four configurations of the final state with a vacancy at the Cu2*p* core orbital (in the one-hole subspace) with weighting factors 0.0560, 0.2241, 0.0037, and 0.0285, while the *z* component is formed by the same transitions with weights of 0.2238, 0.0000, 0.0148, and 0.0000. The energies of these four configurations are 1.9405, 2.1424, 9.8151, and 10.3131 eV, respectively. The profiles of these spectral lines are calculated by the SCF-X_αSW method for the CuO_6^{9-} cluster, which corresponds to the (+3) copper state in the one-electron approximation. The integrated intensity of the polarized lines below the ionization threshold depends only on the occupancies of the corresponding (in accord with the Δm selection rules) vacant *d* orbitals ($x^2 - y^2$ or z^2) in the initial state, whereas the number of multielectron transitions depends on the number of configurations in the final state. In our model, the orthorhombic distortion of the CuO plane is not taken into account, which leads to the absence of the white line in the *z* component of the spectra of the undoped compound, because the d_{z^2} orbital makes no contribution to the initial state; the emergence of the white line in the spectra of the doped compound is due to the mixing of the states $d^8(d_{x^2-y^2} + d_{z^2})$ and $d^9L(d_{z^2})$ with weights $(0.38)^2$ and $(-0.46)^2$, respectively.

The CuL_3 spectra of the singlet state are found by the same procedure. In the *xy*-polarized spectrum, the intensities of transitions to the final configurations are 0.222, 0.001, 0.042, and 0.000, whereas in the *z*-polarized spectrum, they are 0.000, 0.005, 0.000, and 0.002, with the energies of the configurations being 2.139, 2.280, 10.363, and 10.956 eV, respectively. Thus, in the singlet state, as is seen from these data, the density of vacant bound d_{z^2} states is practically zero.

The Cu*K* spectra are also calculated from (7) and (12). For example, the spectrum of undoped La_2CuO_4 is formed from the one-electron spectrum of the Cu$d^{10}\underline{L}$ configuration with a weighting factor of 0.765 and an energy of 2.7 eV and the one-electron spectrum of the Cud^9 configuration with a weight of 0.235 and an energy of 10.6 eV. The spectrum of $LaSrCuO_4$ with the singlet two-hole ground state is also formed from the spectra of two configurations: Cu$d^{10}\underline{LL}$ with a weight of 0.849 and an energy of 2.3 eV and Cu$d^9\underline{L}$ with a weight of 0.144 and an energy of 12.1 eV. The spectrum of $LaSrCuO_4$ with the triplet two-hole ground state is formed from the spectra of three configurations: Cu$d^{10}\underline{LL}$ with a weight of 0.630 and an energy of 3.425 eV, Cu$d^9\underline{L}$ (of an $x^2 - y^2$ character) with a weight of 0.151 and an energy of 11.7 eV, and a combination of Cu$d^9\underline{L}$ (of a z^2 character) and Cud^8, with a weight of 0.219 and an energy of 16.5 eV.

2.5. Low-Concentration Approximation (Independent-Center Model)

In a doped $La_{2-x}Sr_xCuO_4$ crystal, one part of the unit cells has a single hole, while the other part has two holes. The spectra of these partly doped superconductors are calculated under the assumption that the highly correlated two-hole states produced by dopant atoms do not interact with each other, because their concentration is low. In this case, the weighting factors of the one-and two-hole components of the spectra of compounds $La_{2-x}Sr_xCuO_4$ ($x = 0.2$) are taken in accordance with the degree of doping. For example, the spectrum of $La_{1.8}Sr_{0.2}CuO_4$ is formed from the spectrum of La_2CuO_4 with a weight of 0.8 and the spectrum of (singlet or triplet) $LaSrCuO_4$ with a weight of 0.2. The half-widths of the Lorentzian and Gaussian broadening of the CuK_α- and Cu2*p*-XPS spectra are taken to be 0.3 eV.

3. MANIFESTATION OF THE EFFECTS OF STRONG ELECTRON CORRELATIONS IN X-RAY AND ELECTRON SPECTRA

3.1. The Cu2p X-ray Photoelectron Spectra of La_2CuO_4-Type Compounds

As indicated in Section 1, the multiplet structure of the spectra of copper oxides with the Cud^9 configuration is well understood in terms of the multielectron Anderson model and described in detail (see, e.g., [58]). Nonetheless, we would like to cite the typical experimental Cu2*p*-XPS spectra of compounds Cu_2O, CuO, La_2CuO_4, $La_{1.85}Sr_{0.15}CuO_4$ (Fig. 1) [3, 5], and $NaCuO_2$ (Fig. 2) [23].

Figure 9 shows the Cu2*p*-XPS spectra of (a) the one-hole configuration and (b) two-hole configuration

calculated in the extended *p–d* model. According to the calculations, the principal peaks of these two spectra correspond to Cu^{+1}. For example, in the one-hole configuration (Fig. 9a), the occupancy of the Cu$d^{10}\underline{L}$ configuration is $(0.91)^2$, and that of Cud^9 is $(0.42)^2$. In the two-hole configuration, the occupancy of Cu$d^{10}\underline{L}\underline{L}$ is even somewhat higher, $(0.92)^2$; the weight factor of the Cud^8 configuration is negligible, at $(0.05)^2$, while the weights of the two Cu$d^9\underline{L}$ configurations are $(0.37)^2$ and $(0.11)^2$.

It is seen from Fig. 9 that the addition of one more hole leads to the appearance of an extra short-wavelength satellite near 18 eV, associated with transitions to the two Cu$d^9\underline{L}$ configurations with weights $(0.12)^2$ and $(0.81)^2$ and the Cud^8 configurations with a weight of $(0.56)^2$. Thus, these calculations qualitatively support both a growth of the short-wavelength part of the $3d^9$ peak with a doping of La_2CuO_4 and the appearance of an extra satellite in the spectrum of the $NaCuO_2$ compound. The significant differences in the positions of the peaks in $NaCuO_2$ are likely to be due to the fact that the Cud^8 configurations are practically absent in $NaCuO_2$ [90] and only the Cu$d^9\underline{L}$ configuration is responsible for the formation of the principal peak; hence, copper is in the bivalent state in this compound. As for the energy spacing between these two satellites in La_2CuO_4, its overestimation by roughly 3 eV is due, in our opinion, to the rather inexact determination of the *p–d*-model parameters.

If the spin–orbit splitting of the core 2*p* energy level and the effect of doping on the spectra in the independent-center approximation (Fig. 10) are taken into account, then, in the spectrum of $La_{1.8}Sr_{0.2}CuO_4$, the principal peak depending on the occupancy of the Cu$d^{10}\underline{L}$ configuration has a feebly marked (in proportion to the degree of doping) asymmetric short-wavelength structure (with a peak at 17 eV) associated with the energy separation of the Cu$d^{10}\underline{L}$ and Cu$d^{10}\underline{L}\underline{L}$ cluster configurations with the formal (+2) and (+3) oxidation levels of copper. In our opinion, a comparison of our results and the experimental spectrum [3] (Figs. 1, 2) lends credence to this prediction.

For the most part, the results we obtained are similar to the calculations of the Cu2*p* XPS in [58], with the essential difference being that the high-energy satellite separated by 14 eV from the principal line is absent in [58], which is due, in our opinion, to the fact that we perform the complete diagonalization of the Hamiltonian, including all two-particle states, whereas in [58], the diagonalization is carried out numerically in a given, less complete, basis.

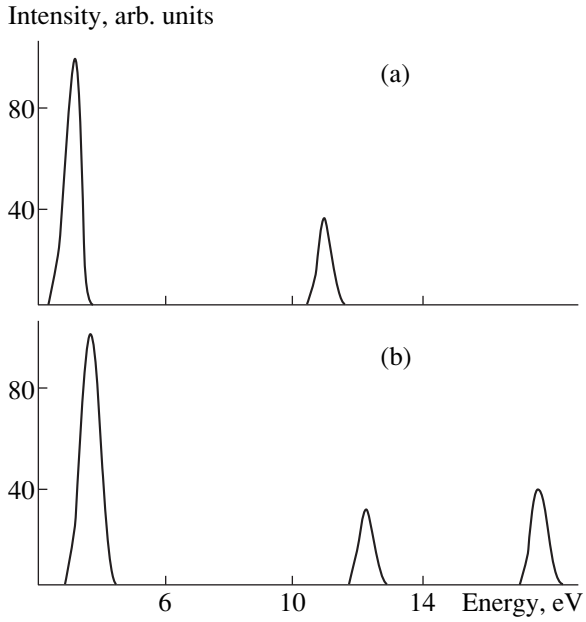

Fig. 9. Theoretical Cu2*p* X-ray photoelectron spectra of compounds (a) La_2CuO_4 and (b) $LaSrCuO_4$ without spin–orbit splitting of the Cu2*p* orbital.

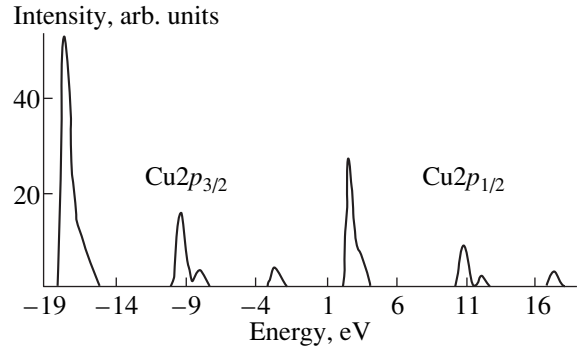

Fig. 10. Theoretical Cu2*p* X-ray photoelectron spectrum of the $La_{1.8}Sr_{0.2}CuO_4$ compound (including the spin–orbit splitting of the 2*p* orbital of copper, $\Delta_\varepsilon = 20$ eV), calculated in the independent-center approximation.

3.2. The CuK$_\alpha$ Spectra of La$_2$CuO$_4$-Type Compounds

As mentioned in Section 1, the theoretical spectra of systems with one hole are described in detail in [36, 37]. In these spectra, there is a faint satellite depending on the density of the Cud^9 configurations and lying 0.4 eV above the principal peak, which depends on the density of Cu$d^{10}\underline{L}$ state in the 1*s*- and 2*p*-hole configurations. As shown in [37], the shift of the K_α line of copper cannot be measured, using the Larson model, without separating the satellite structure configurations.

In our case, the addition of one more hole to the cluster leads to the change in the nature of the principal peak (Fig. 11), which now depends, for the most part,

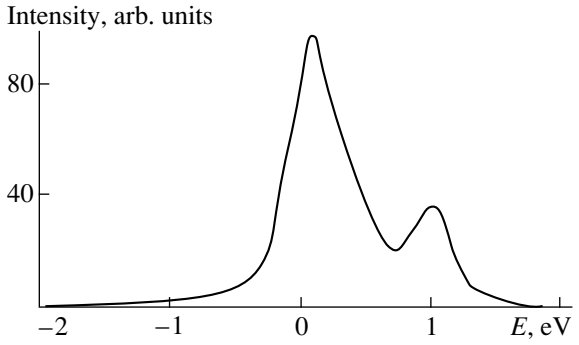

Fig. 11. Theoretical CuK_α spectrum of the two-hole configuration corresponding to the $LaSrCuO_4$ compound.

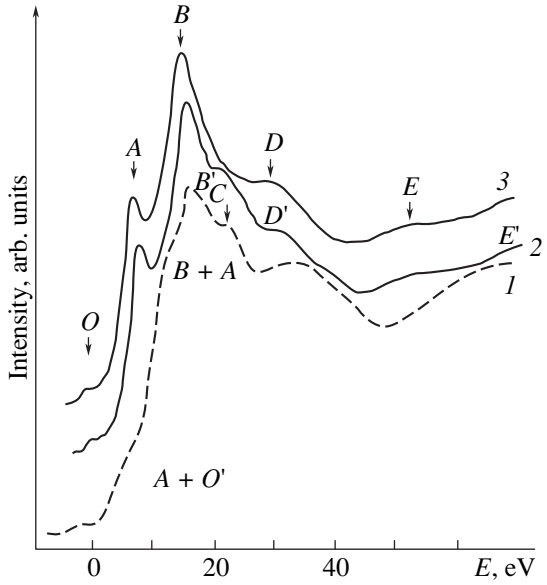

Fig. 12. Experimental [28] (*1*), theoretical Cu*K* (including multielectron effects) (*2*), and theoretical one-electron (*3*) absorption spectra of La_2CuO_4. Peaks *O*, *A*, *B*, *D*, and *E* correspond to the principal spectral line (configuration $d^{10}\underline{L}$), while peaks *O*', *A*', *B*', *D*', and *E*' correspond to the shake-up satellite (configuration d^9), separated from the principal line by 7.8 eV.

on the density of the Cu$d^{10}\underline{LL}$ configurations of the ground, intermediate, and final 1*s* and 2*p* hole states. The faint satellite lying 0.4 eV above the principal peak now reflects the density of the Cu$d^9\underline{L}$ configurations, while the new short-wavelength intense satellite at 1 eV is due to the two Cu$d^9\underline{L}$ configurations and the one Cud^8 configuration with a weight of $(0.56)^2 + (0.57)^2$. When the spin–orbit splitting of the core 2*p* orbital of copper and the superposition of the two-hole and one-hole spectra (in the independent-center model) are taken into account, there appear asymmetry and a faint shoulder on the short-wavelength side of the principal peak.

3.3. The Ground Terms of the Initial and Final X-ray States of the CuO_4 Cluster

The weights of the d^9 and $d^{10}\underline{L}$ configurations of the undoped CuO_4 unit cell in La_2CuO_4 are 69 and 31%, respectively. Thus, the copper ion in this cell is basically in the common Cu^{+2} oxidation state. Doping does not change this picture; the dominant configuration of the CuO_4 unit cell of the completely doped $LaSrCuO_4$ compound is the $d^9\underline{L}$ configuration with a weight of 57% (the contribution from the $d_{x^2-y^2}$ state is 36% and that from the d_{z^2} state is 21%), while the weight of the $d^9\underline{LL}$ configuration is 28% and that of d^8 is 14%.

The creation of an X-ray core (1*s* or 2*p*) hole leads to a dramatic rearrangement of the electronic structure of both doped and undoped unit cells. In this case, the weights of the d^9 and $d^{10}\underline{L}$ configurations of the undoped CuO_4 unit cell of La_2CuO_4 are 18 and 82%, respectively. Thus, the oxidation level of copper is changed and equals +1. The same picture takes place in doped CuO_4 unit cells, in which the weight of the $d^{10}\underline{LL}$ configuration is 85%, while that of $d^9\underline{L}$ is 15% (14% of $d_{x^2-y^2}$ and 1% of d_{z^2}). The weight of the d^8 configuration is negligible, only 0.3%.

3.4. The CuK Absorption Spectra of $La_{2-x}Sr_xCuO_4$

There is some direct experimental evidence that strong electron correlations affect the Cu*K* X-ray absorption spectra of La_2CuO_4 [91]. The mechanism of the formation of these spectra was investigated in detail by using various versions of the nonempirical one-electron multiple-scattering method [24–27], and all features were adequately described, except for the peak *C*, which lies 7 eV above the principal peak. The former peak appeared only in the *xy*-polarized spectra when the cluster size was as large as 50–60 atoms [25–27], whereas, experimentally, this feature is also observed in the *z* polarization [91].

When one more vacancy per unit cell is added by doping, contributions from the Cud^8, Cu$d^9\underline{L}$, and the Cu$d^{10}\underline{LL}$ configurations appear. This leads to significantly more complicated Cu*K* absorption spectra associated with the electronic states produced by doping of HTSC compounds [28].

In order to study the effect of strong electron correlations on the Cu*K* X-ray absorption spectra, we completely diagonalize the multiband *p*–*d*-model Hamiltonian of the CuO_4 cluster in the sudden-perturbation approximation described in Section 2. The matrix ele-

ments of X-ray-induced transitions $1s \longrightarrow p(\varepsilon)$ are calculated for the CuO_6^{10-} and CuO_6^{9-} clusters by the nonempirical SCF-X_αSW method. The final spectra are constructed using the spectral line profiles as calculated by the one-electron method and the weight factors and energies of configurations as calculated in the many-band *p–d* model. The spectrum of completely doped $LaSrCuO_4$ is calculated for both the singlet and triplet two-hole states.

3.5. Discussion of Results

Figure 12 shows the experimental [28] and theoretical one-electron Cu*K* spectra of La_2CuO_4. It is seen that both the positions and the relative intensities of the peaks of the calculated spectrum, including multielectron effects, correlate well with those of the experimental spectrum, excepting perhaps the long-wavelength range of the spectra near peak *A*. It has been pointed out in the literature that some discrepancy in this range is due to the small size of the CuO_6^{10-} cluster for which the theoretical peak *A* was calculated [25–27].

The calculations showed that the principal spectral line in the Cu*K* spectrum corresponds to the $d^{10}\underline{L}$ configuration with a weight of $(0.88)^2$ (peaks *O*, *A*, *B*, *D*, and *E*), whereas the single intense short-wavelength shake-up satellite (peak *C* in the experimental spectrum and peak *B*' in the theoretical one in Fig. 12), separated by an energy of 7.8 eV from the principal peak, is associated with the d^9 configuration (peaks *O*', *A*', *B*', *D*', and *E*'). Therefore, the experimental peak *C* should be correlated with the theoretical peak *B*'. This peak is due to photoelectron scattering by surrounding atoms in La_2CuO_4, as is indicated in the literature [25–27], and is also associated with the Cud^9 configuration in this compound.

The shape of the experimental Cu*K* spectrum of dopant-produced states in $LaSrCuO_4$ ("trivalent copper") is significantly more complex [28] (Fig. 13). A comparison of the experimental [28] (curve *1*) and theoretical Cu*K* spectra of $LaSrCuO_4$ with the singlet (curve *3*) and triplet (curve *2*) ground states shows that the two-hole ground state of $LaSrCuO_4$ in the doped $La_{2-x}Sr_xCuO_4$ system is the triplet. The principal line in this spectrum (peaks *O*, *A*, *B*, *D*, and *E*) is associated with the $d^{10}\underline{L}\underline{L}$ configuration with a weight of $(0.91)^2$ mixed with small amounts of states $d^9\underline{L}$ ($x^2 - y^2$, with a weight of $(0.39)^2$, and z^2 with a weight of $(0.12)^2$). The first satellite (peaks *O*', *A*', *B*', *D*', and *E*') is principally associated with the $d^9\underline{L}$ state of an $x^2 - y^2$ character with a weight of $(0.90)^2$, mixed with a small amount of $d^{10}\underline{L}\underline{L}$ (with a weight of $(0.39)^2$). The second satellite (peaks *O*", *A*", *B*", *D*", and *E*") depends on the density of configurations $d^9\underline{L}$ (z^2), having a weight of $(0.81)^2$, and d^8, having a weight of $(0.57)^2$, mixed with a small amount of $d^9\underline{L}$ ($x^2 - y^2$) with a weight of $(0.12)^2$. The symbols above the experimental curve in Fig. 13 indicate the correspondence between peaks and configurations. Some discrepancies observed for the relative intensities and positions of peaks *A*' and *B*' are associated with the overestimation of the relative intensity of peak *A* in the one-electron calculation, which leads to some distortion of the final spectrum.

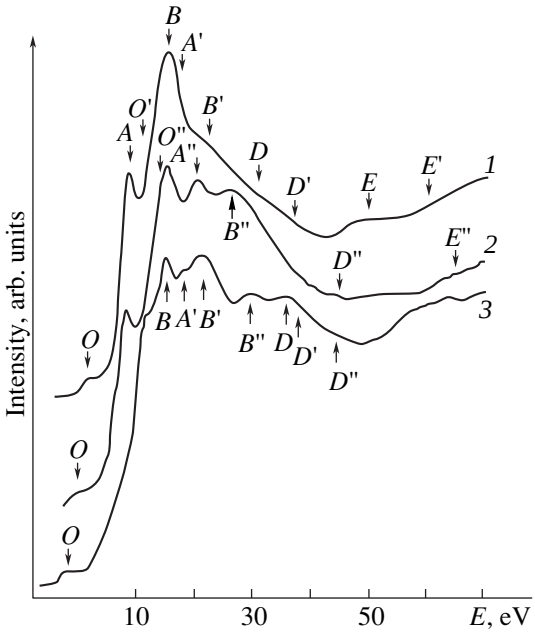

Fig. 13. Experimental [28] (*1*) and theoretical Cu*K* X-ray absorption spectra for dopant-produced two-hole states with the triplet (*2*) and singlet (*3*) ground states. Peaks *O*, *A*, *B*, *D*, and *E* correspond to the principal spectral line (the $d^{10}\underline{L}\underline{L}$ state); peaks *O*', *A*', *B*', *D*', and *E*' correspond to the first satellite (the $d^9\underline{L}$ ($x^2 - y^2$) state); and peaks *O*", *A*", *B*", *D*", and *E*" correspond to the second satellite (the $d^9\underline{L}$ (z^2) and d^8 states).

3.6. The Influence of Strong Electron Correlations of the CuL_3 X-ray Absorption Spectra of $La_{2-x}Sr_xCuO_4$

The scheme for calculating the CuL_3 absorption spectra was described in detail in Section 2. In the $La_{2-x}Sr_xCuO_4$ system with $x = 0$ (with one electron vacancy per formula unit), as was shown in [32], there occurs only one X-ray-induced transition, $2p^6d^9_{x^2-y^2} \longrightarrow 2p^5d^{10}$, although the initial state consists of two d^9-type and two $d^{10}\underline{L}$-type configurations by virtue of the hybridization of vacant states. In the case of $x > 0$, there appear contributions from the Cud^8, Cu$d^9\underline{L}$, and Cu$d^{10}\underline{L}\underline{L}$ configurations, due to which the multielectron effects become much stronger and the CuL_3 spec-

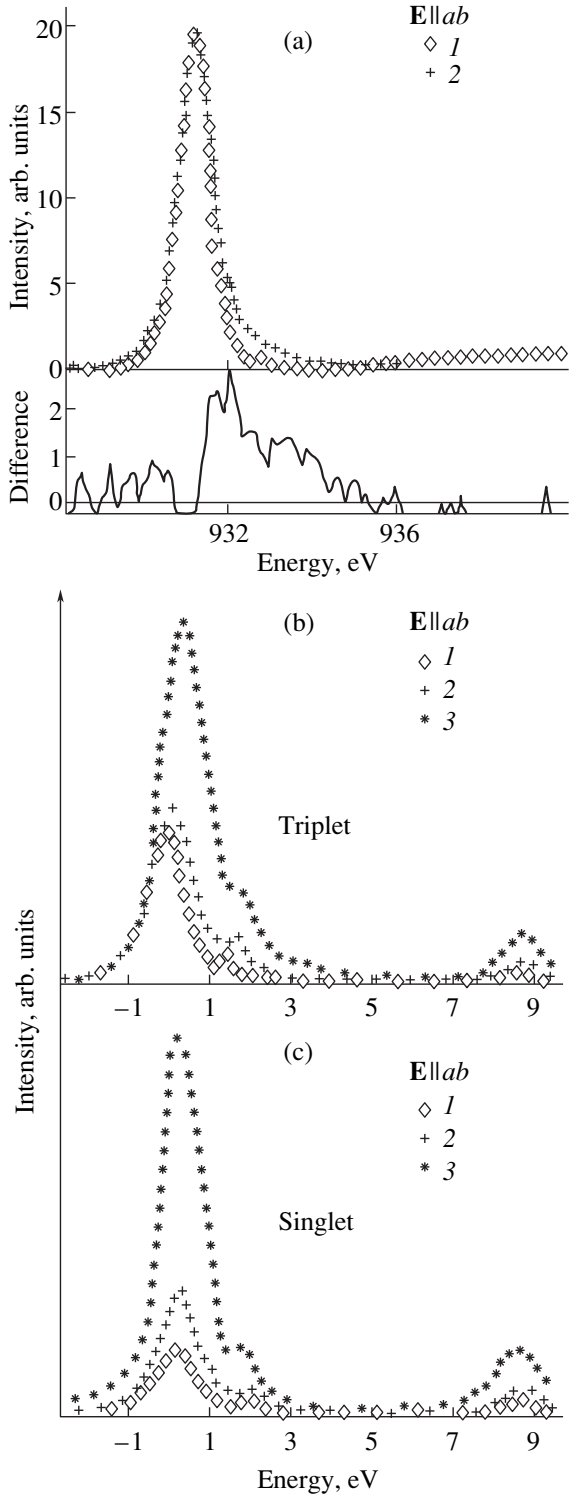

Fig. 14. (a) Experimental *xy*-polarized CuL_3 X-ray absorption spectra of (*1*) La_2CuO_4 and (*2*) $La_{1.92}Sr_{0.08}CuO_4$ [2]; (b) theoretical *xy*-polarized spectra of compounds (*1*) La_2CuO_4, (*2*) $La_{1.92}Sr_{0.08}CuO_4$, and (*3*) $LaSrCuO_4$ for when the two-hole ground state is the triplet; and (c) theoretical *xy*-polarized spectra of compounds (*1*) La_2CuO_4, (*2*) $La_{1.92}Sr_{0.08}CuO_4$, and (*3*) $LaSrCuO_4$ for when the two-hole state is the singlet; **E** ∥ *ab*.

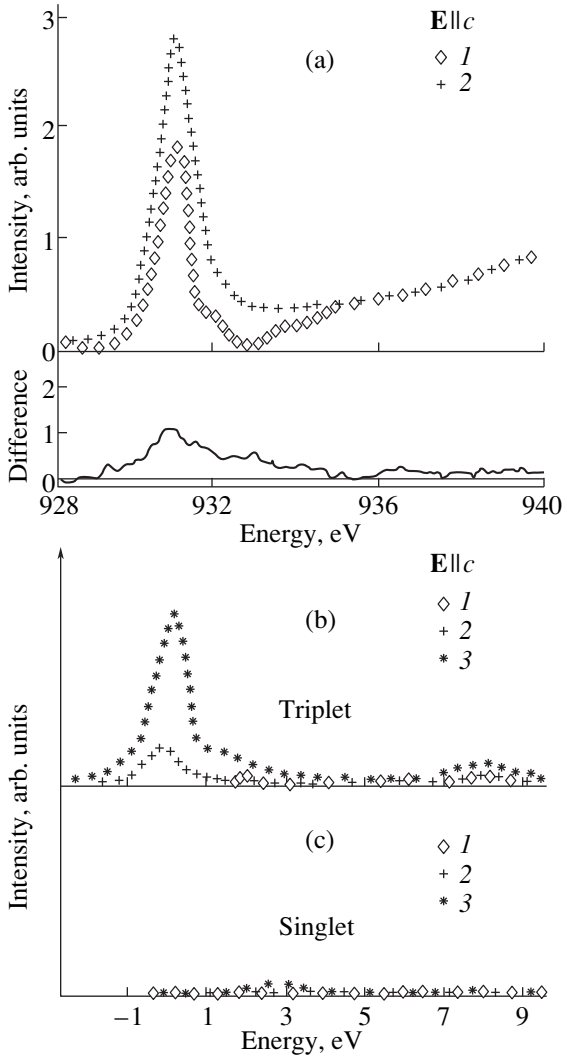

Fig. 15. (a) Experimental *z*-polarized CuL_3 X-ray absorption spectra of (*1*) La_2CuO_4 and (2) $La_{1.92}Sr_{0.08}CuO_4$ [2]; (b) theoretical *z*-polarized spectra of compounds (*1*) La_2CuO_4, (*2*) $La_{1.92}Sr_{0.08}CuO_4$, and (*3*) $LaSrCuO_4$ for when the two-hole ground state is the triplet; and (c) theoretical *z*-polarized spectra of compounds (*1*) La_2CuO_4, (*2*) $La_{1.92}Sr_{0.08}CuO_4$, and (*3*) $LaSrCuO_4$ for when the two-hole ground state is the singlet; **E** ∥ *c*.

tra of dopant-produced electronic states of doped compounds differ noticeably from those of undoped ones (in particular, shake-up satellites appear near the white line [2, 32, 33]).

Figure 14a presents the experimental CuL_3 spectra of La_2CuO_4 and $La_{1.92}Sr_{0.08}CuO_4$ [2] for the *xy* polarization, while the theoretical *xy*-polarized spectra of the La_2CuO_4, $LaSrCuO_4$, and $La_{1.92}Sr_{0.08}CuO_4$ compounds are shown in Fig. 14b for when the two-hole ground state is the triplet, and in Fig. 14c for when this state is the singlet.

Figure 15a presents the experimental CuL_3 spectra of La_2CuO_4 and $La_{1.92}Sr_{0.08}CuO_4$ [2] for the *z* polarization, while the theoretical *z*-polarized spectra of the La_2CuO_4, $LaSrCuO_4$, and $La_{1.92}Sr_{0.08}CuO_4$ compounds are shown in Fig. 15b for the case where the two-hole ground state is the triplet and in Fig. 15c for the case where this state is the singlet.

In both the experimental and theoretical *xy*-polarized spectra of the undoped La_2CuO_4 compound (Fig. 14), there are no nondiagram spectral lines (the electronic transitions that cannot be described in terms of the crystal-field theory in the first approximation) below the ionization threshold. However, in the experimental *z*-polarized spectrum (Fig. 15), a fairly intense white line is observed, which is absent in the corresponding theoretical spectrum. This difference is due to the fact that, in this paper, no account is taken of the orthorhombic distortion of the CuO_2 plane, which, as was shown in [92], is responsible for this effect. The shape of the line above the ionization threshold in both the *z*- and *xy*-polarized spectra is described adequately, as in the case of the spectra calculated in the one-electron approximation [27].

The principal difference between the experimental spectra of doped and undoped compounds is that, in the former case, the intensity of the white line becomes much higher in the *z* polarization (Fig. 15). The absence of the white line in the theoretical *z*-polarized spectrum of a doped compound with the singlet ground state and its presence in the case of the triplet ground state (Fig. 15) suggests that, in the unit cell with two electron vacancies, the ground state is the triplet. In this case, the white line is associated with transitions from the ground state to a final state with a Cu2*p* vacancy and with appreciably populated d_{z^2} states of the $d^8(d_{x^2-y^2} + d_{z^2})$ and $d^9\underline{L}(d_{z^2})$ orbitals (with weights of $(0.38)^2$ and $(-0.46)^2$, respectively) with a transition energy of 1.94 eV and an intensity of 0.2238. The transition intensity of the white line with the *z* polarization for the configuration being next in energy is equal to zero.

Our model adequately describes the faint long-wavelength satellite in the *xy* polarization, which is associated with the lowest energy configuration of the final state with a core 2*p* vacancy (the transition intensity 0.0560) and is situated 0.4 eV below the white line in the experimental spectrum (Fig. 14) [2]. The *xy*-polarized white line for the triplet state is associated with the configuration that is next in energy and for which the transition energy is 2.14 eV and the intensity is 0.2241. The transition intensities to the next two high-energy configurations (for which the transition energies are 9.82 and 10.31 eV, respectively) are virtually zero in these spectra, and the corresponding white lines are practically absent above the ionization threshold. In the range above the threshold, the spectra are largely composed of the lines due to the first two configurations. The small energy separation between these spectral lines and the large (compared to that of the white line) half-widths of the features lead to some flattening of the spectra in the positive energy range. In our calculations, in contrast to those in [30], the peak corresponding to the *s* states (at about 8 eV) in the range above the ionization threshold has a noticeable intensity, which is due, in our opinion, to the cluster effect.

CONCLUSIONS

Analysis of the literature showed that a great body of experimental data give evidence of the rather dramatic effect of strong electron correlations on the electronic structure of high-T_c superconductors and, in particular, on the structure of vacant electronic states. For example, the investigation of the X-ray absorption spectra allowed one to separate out two-particle contributions due to doping, and it was shown that one dopant atom interacts with two copper centers and produces vacant electronic states of a Cud_{z^2} character.

Theoretical one-electron and multielectron calculations of the electronic structure of the key objects were performed, but, as a rule, they were not accompanied by theoretical modeling of the available spectroscopic measurements. It became clear that most of the experimental X-ray and electron spectra could not be directly and unambiguously interpreted. This was due to the fact that the principal features of the electronic structure of high-T_c superconductors are determined by strong electron correlations. Only some experimental data have been adequately described in terms of the current theoretical models. These data were obtained, for the most part, for insulating phases, whereas no spectra of dopant-produced two-hole states have been theoretically investigated up to now. For treating the spectral properties of a material with a strongly correlated electron system, a multielectron theory of X-ray and X-ray electron spectra has been developed on the basis of the sudden-perturbation model. This theory allowed one to describe a number of key spectral characteristics of the compounds in question in a unified way. The X-ray and electronic spectra were represented in the form of convolution of the spectrum of one-electron transitions to vacant orbitals both below and above the ionization threshold and the spectrum of multielectron transitions within the system of valence electrons.

In all the spectra investigated (except for the CuL_3 absorption spectrum), the principal spectral lines correspond either to the Cu$d^{10}\underline{L}$ (for the undoped unit cell) or to the Cu$d^{10}\underline{LL}$ (for the doped unit cell) configuration. In the spectra of undoped centers, the satellite structures are determined by the contributions from the Cud^9 configurations. Doping leads to more complicated spectra, which contain satellites depending on the density of the Cu$d^9\underline{L}$ configurations. In all cases considered, the contribution from the Cud^8 two-hole con-

figurations is small. The white line of the CuL_3 spectrum of undoped and doped unit cells corresponds to the Cud^9 and Cu$d^9\underline{L}$ configurations, respectively. Doping leads to an increase in the occupancy of the Cud_{z^2} orbitals, which in turn results in an increase of the intensity of the z-polarized CuL_3 spectrum.

ACKNOWLEDGMENTS

This work was supported by the Scientific Council on the HTSC Problem and by the "Vysokotemperaturnaya sverkhprovodimost" State Program.

REFERENCES

1. E. E. Alp, G. K. Shenoy, D. G. Hinks, *et al.*, Phys. Rev. B **35**, 7199 (1987).
2. M. Pompa, C. Li, A. Bianconi, *et al.*, Physica C **184**, 51 (1991).
3. J. Fuggle, J. Fink, and N. Nucker, Int. J. Mod. Phys. B **5**, 1185 (1988).
4. A. Fujimori, E. Takayama-Myromachi, Y. Uchida, *et al.*, Phys. Rev. B **35**, 8814 (1987).
5. F. Al Shamma and J. C. Fuggle, Physica C **169**, 325 (1990).
6. A. Bianconi, J. Budnik, B. Chamberland, *et al.*, Physica C **153–155**, 115 (1988).
7. N. Nucker, J. Fink, B. Renker, *et al.*, Z. Phys. B **67**, 9 (1987).
8. P. Steiner, J. Albers, V. Kinsinger, *et al.*, Z. Phys. B **66**, 275 (1987).
9. P. Steiner, R. Courth, V. Kinsinger, *et al.*, Appl. Phys. A **44**, 75 (1987).
10. D. D. Sarma, Phys. Rev. B **37**, 7948 (1988).
11. D. E. Ramaker, N. H. Turner, J. S. Murday, *et al.*, Phys. Rev. B **36**, 5672 (1987).
12. A. Ueda, Y. Okamoto, and T. Imanaka, Chem. Express **3**, 723 (1988).
13. H. Ishii, T. Koschizawa, H. Kataura, *et al.*, Jpn. J. Appl. Phys. **28**, L1952 (1989).
14. G. van der Laan, C. Westra, C. Haas, *et al.*, Phys. Rev. B **23**, 4369 (1981).
15. G. van der Laan, G. A. Sawatzky, C. Haas, *et al.*, Phys. Rev. B **20**, 4287 (1979).
16. R. Manne and T. Aberg, Chem. Phys. Lett. **7**, 282 (1970).
17. A. Kotani and Y. Toyozawa, Jpn. J. Phys. **35**, 1073 (1973).
18. A. Kotani and Y. Toyozawa, Jpn. J. Phys. **37**, 912 (1974).
19. O. Gunnarsson and K. Schönhammer, Phys. Rev. Lett. **50**, 604 (1983).
20. O. Gunnarsson and K. Schönhammer, Phys. Rev. B **28**, 4315 (1983).
21. O. Gunnarsson and K. Schönhammer, Phys. Rev. B **31**, 4815 (1985).
22. J. C. Fuggle, M. Campagna, Z. Zolnierek, *et al.*, Phys. Rev. Lett. **45**, 1597 (1980).
23. P. Steiner, V. Kinsinger, I. Sander, *et al.*, Z. Phys. B: Condens. Matter **67**, 467 (1987).
24. P. V. Avramov, A. V. Kondratenko, S. Ph. Ruzankin, *et al.*, Preprint No. 89-05 (Inst. of Inorg. Chem., Acad. of Sci. of the USSR, Siberian Branch, 1989).
25. J. Guo, D. E. Ellis, G. L. Goodman, *et al.*, Phys. Rev. B **41**, 82 (1990).
26. C. Li, M. Pompa, A. C. Castellano, *et al.*, Physica C **175**, 369 (1991).
27. P. V. Avramov, S. Ph. Ruzankin, and G. M. Zhidomorov, Phys. Rev. B **46**, 6495 (1992).
28. N. Kosugi, Y. Tokura, H. Takagi, *et al.*, Phys. Rev. B **41**, 131 (1990).
29. Y. Seino, A. Kotani, and A. Biankoni, J. Phys. Soc. Jpn. **59**, 815 (1990).
30. M. Pompa, P. Castricci, C. Li, *et al.*, Physica C **184**, 102 (1991).
31. O. Strebel, G. Kaindl, A. Kolodziejcyk, *et al.*, J. Magn. Magn. Mater. **76–77**, 597 (1988).
32. Y. Seino, K. Okada, and A. Kotani, J. Phys. Soc. Jpn. **59**, 1384 (1990).
33. A. Bianconi, A. C. Castellano, M. De Santis, *et al.*, Solid State Commun. **63**, 1009 (1987).
34. S. Kishida, H. Tokutaka, S. Nakanishi, *et al.*, Jpn. J. Appl. Phys. **28**, L949 (1989).
35. E. Z. Kurmaev, V. I. Nefedov, and L. D. Finkelstain, Int. J. Mod. Phys. B **2**, 393 (1988).
36. M. S. Osadchiĭ, V. V. Murakhtanov, É. S. Fomin, *et al.*, Zh. Éksp. Teor. Fiz. **101**, 1259 (1992) [Sov. Phys. JETP **74**, 674 (1992)].
37. L. N. Mazalov, D. M. Tolstyakov, V. V. Murakhtanov, *et al.*, Zh. Strukt. Khim. **30**, 78 (1989).
38. J. Redinger, Yu. J. Freeman, and A. J. Weinberg, Phys. Lett. A **124**, 463 (1987).
39. B. Reihl, T. Reisesterer, J. D. Bednorz, *et al.*, Phys. Rev. B **35**, 8804 (1987).
40. J. C. Fuggle, P. J. W. Weijs, R. Schoorl, *et al.*, Phys. Rev. B **37**, 123 (1988).
41. H. Chen, J. Callaway, and P. K. Misra, Phys. Rev. B **36**, 8863 (1987).
42. V. I. Anisimov, V.R. Galakhov, V. A. Gubanov, *et al.*, Fiz. Met. Metalloved. **65**, 204 (1988).
43. W. M. Temmerman, G. M. Stocks, P. J. Durham, *et al.*, Preprint No. DL/SCI/P551T (Daresbury Lab., UK, 1987).
44. L. F. Mattheis, Phys. Rev. Lett. **58**, 1028 (1987).
45. J. Fink, N. Nucker, H. A. Romberg, *et al.*, J. Res. Develop. **33**, 372 (1989).
46. S. Ushida, Int. J. Mod. Phys. B **2**, 181 (1988).
47. V. I. Anisimov, M. A. Korotin, and I. V. Afanasyev, Physica C **161**, 59 (1989).
48. V. I. Anisimov, M. A. Korotin, and E. Z. Kurmaev, J. Phys.: Condens. Matter **2**, 3973 (1990).
49. M. A. Korotin, V. I. Anisimov, S. M. Butorin, *et al.*, Mater. Lett. **10**, 34 (1990).
50. J. Zaanen, G. A. Sawatzky, and J. W. Allen, Phys. Rev. Lett. **55**, 418 (1985).
51. I. I. Mazin, Usp. Fiz. Nauk **158**, 155 (1989) [Sov. Phys. Usp. **32**, 469 (1989)].
52. J. Zaanen, O. Jepsen, O. Gunnarsson, *et al.*, Physica C **153–155**, 1636 (1988).

53. W. Brenig, Phys. Rep. **251**, 153 (1995).
54. K. Okada and A. Kotani, J. Phys. Soc. Jpn. **58**, 1095 (1989).
55. A. Fujimori, Phys. Rev. B **39**, 793 (1989).
56. D. Sarma and S. G. Ovchinnikov, Phys. Rev. B **42**, 6817 (1990).
57. M. S. Osadchiĭ, V. V. Murakhtanov, É. S. Fomin, *et al.*, Zh. Strukt. Khim. **30**, 78 (1989).
58. F. C. Zhang and T. M. Rice, Phys. Rev. B **37**, 3759 (1988).
59. R. A. Bair and W. A. Goddard III, Phys. Rev. B **22**, 2767 (1980).
60. A. V. Kondratenko and L. S. Cederbaum, Phys. Rev. B **43**, 10595 (1991).
61. M. Eto and H. Kamimura, J. Phys. Soc. Jpn. 60, 2311 (1991).
62. V. J. Emery, Phys. Rev. Lett. **58**, 2794 (1987).
63. C. M. Varma, S. Schmitt-Rink, and E. Abrahams, Solid State Commun. **62**, 681 (1987).
64. Yu. B. Gaididei and V. B. Loktev, Phys. Status Solidi **147**, 308 (1988).
65. S. G. Ovchinnikov, Zh. Éksp. Teor. Fiz. **102**, 127 (1992) [Sov. Phys. JETP **75**, 67 (1992)].
66. S. G. Ovchinnikov, Usp. Fiz. Nauk **167**, 1043 (1997) [Phys. Usp. **40**, 1095 (1997)].
67. S. G. Ovchinnikov and I. S. Sandalov, Physica C **161**, 607 (1989).
68. S. G. Ovchinnikov, Mod. Phys. Lett. B **5**, 531 (1991).
69. P. V. Avramov and S. G. Ovchinnikov, Physica C **278**, 94 (1997).
70. Z.-X. Shen, J. W. Allen, J. J. Yeh, *et al.*, Phys. Rev. B **36**, 8414 (1987).
71. R. Zanoni, Y. Chang, M. Tang, *et al.*, Phys. Rev. B **38**, 11832 (1988).
72. H. Namatame, A. Fujimori, Y. Tokura, *et al.*, Phys. Rev. B **41**, 7205 (1990).
73. F. Bloch, Phys. Rev. **48**, 187 (1935).
74. R. D. Richtmyer, Phys. Rev. **49**, 1 (1936).
75. F. L. Feinberg, Phys. **IV**, 423 (1941).
76. A. J. Migdal, Phys. **IV**, 449 (1941).
77. V. P. Sachenko and V. F. Demekhin, Zh. Éksp. Teor. Fiz. **49**, 765 (1965).
78. L. D. Landau and E. M. Lifshitz, *Quantum Mechanics: Nonrelativistic Theory* (Fizmatgiz, Moscow, 1963).
79. D. I. Blokhintsev, *Principles of Quantum Mechanics* (Nauka, Moscow, 1976).
80. L. N. Mazalov, V. D. Yumatov, and V. V. Murakhtanov, *X-ray Spectra of Molecules* (Nauka, Novosibirsk, 1977).
81. S. Larson, Chem. Phys. Lett. **32**, 401 (1975).
82. S. Larson, Chem. Phys. Lett. **40**, 362 (1976).
83. S. Larson, Phys. Scripta **21**, 558 (1980).
84. S. Larson and M. Braga, Chem. Phys. Lett. **48**, 596 (1977).
85. F. W. Kutzler, C. R. Natoli, D. K. Misemer, *et al.*, J. Chem. Phys. **73**, 3274 (1980).
86. S. F. Ruzankin, Zh. Strukt. Khim. **20**, 953 (1979).
87. S. F. Ruzankin, V. I. Nemanova, and A. V. Kondratenko, Zh. Strukt. Khim. **27**, 162 (1986).
88. J. D. Jorgensen, H.-B. Schüttler, and D. G. Hinks, Phys. Rev. Lett. **58**, 1024 (1987).
89. P. Bordet, C. Chailont, J. J. Capponi, *et al.*, Nature **327**, 687 (1987).
90. D. Khomskii, *The International Conference on Strongly Correlated Electron Systems 68* (Amsterdam, 1994).
91. H. Oyanagi, K. Oka, H. Unoki, *et al.*, Physica B **158**, 436 (1989).
92. S. G. Ovchinnikov, Fiz. Tverd. Tela (Leningrad) **35**, 617 (1993) [Phys. Solid State **35**, 315 (1993)].

Translated by Yu. Epifanov